THE ANATOMICAL RECORD 290:1459–1479 (2007)

Neuroanatomy of the Subadult and Fetal Brain of the Atlantic White-Sided Dolphin (*Lagenorhynchus acutus*) from In Situ Magnetic Resonance Images

ERIC W. MONTIE,[1,2]* GERALD E. SCHNEIDER,[3] DARLENE R. KETTEN,[1] LORI MARINO,[4] KATIE E. TOUHEY,[5] AND MARK E. HAHN[1]

[1]Woods Hole Oceanographic Institution, Woods Hole, Massachusetts
[2]College of Marine Science, University of South Florida, St. Petersburg, Florida
[3]Department of Brain and Cognitive Sciences, MIT, Cambridge, Massachusetts
[4]Neuroscience and Behavioral Biology Program, Emory University, Atlanta, Georgia
[5]Cape Cod Stranding Network, Buzzards Bay, Massachusetts

ABSTRACT

This article provides the first anatomically labeled, magnetic resonance imaging (MRI) -based atlas of the subadult and fetal Atlantic white-sided dolphin (*Lagenorhynchus acutus*) brain. It differs from previous MRI-based atlases of cetaceans in that it was created from images of fresh, postmortem brains in situ rather than extracted, formalin-fixed brains. The in situ images displayed the classic hallmarks of odontocete brains: fore-shortened orbital lobes and pronounced temporal width. Olfactory structures were absent and auditory regions (e.g., temporal lobes and inferior colliculi) were enlarged. In the subadult and fetal postmortem MRI scans, the hippocampus was identifiable, despite the relatively small size of this structure in cetaceans. The white matter tracts of the fetal hindbrain and cerebellum were pronounced, but in the telencephalon, the white matter tracts were much less distinct, consistent with less myelin. The white matter tracts of the auditory pathways in the fetal brains were myelinated, as shown by the T2 hypointensity signals for the inferior colliculus, cochlear nuclei, and trapezoid bodies. This finding is consistent with hearing and auditory processing regions maturing in utero in *L. acutus*, as has been observed for most mammals. In situ MRI scanning of fresh, postmortem specimens can be used not only to study the evolution and developmental patterns of cetacean brains but also to investigate the impacts of natural toxins (such as domoic acid), anthropogenic chemicals (such as polychlorinated biphenyls, polybrominated diphenyl ethers, and their hydroxylated metabolites), biological agents (parasites), and noise on the central nervous system of marine mammal species. Anat Rec, 290:1459–1479, 2007.

Key words: Atlantic white-sided dolphin; *Lagenorhynchus acutus*; odontocete; fetal; delphinid; cetacea; brain; MRI

Grant sponsor: Environmental Protection Agency; Grant number: U-91616101-2; Grant sponsor: The National Woman's Farm and Garden Association; Grant sponsor: Shields MRI and CT of Cape Cod; Grant sponsor: The Quebec Labrador Fund/Atlantic Center for the Environment; Grant sponsor: Woods Hole Oceanographic Institution Academic Programs Office; Grant sponsor: Office of Naval Research; Grant sponsor: The Sawyer Endowment; Grant sponsor: NOAA Fisheries Marine Mammal Health and Stranding Response Program; Grant sponsor: Walter A. and Hope Noyes Smith.

*Correspondence to: Eric W. Montie, College of Marine Science, University of South Florida, 140 Seventh Avenue, South, St. Petersburg, FL 33701-5016. Fax: 727-553-1189.
E-mail: emontie@marine.usf.edu

Received 8 June 2007; Accepted 31 August 2007
DOI 10.1002/ar.20612
Published online 24 October 2007 in Wiley InterScience (www.interscience.wiley.com).

Odontocetes (toothed whales, dolphins, and porpoises) have undergone unique anatomical adaptations to an aquatic environment. One significant modification is in brain size. In fact, several odontocete species have encephalization quotients (a measure of relative brain size) that are second only to those of modern humans (Ridgway and Brownson, 1984; Marino, 1998). Several studies of odontocete neuroanatomy, primarily from histology and gross dissection, have been completed, as reviewed by Morgane et al. (1986) and Ridgway (1990). However, few studies have focused on odontocete prenatal neuroanatomy or neuroanatomical changes during ontogeny (Marino et al., 2001b).

Magnetic resonance imaging (MRI) has been used recently to study the neuroanatomy of the beluga whale (*Delphinapterus leucas*; Marino et al., 2001a), the fetal common dolphin (*Delphinus delphis*; Marino et al., 2001b), the bottlenose dolphin (*Tursiops truncatus*; Marino et al., 2001c), the harbor porpoise (*Phocoena phocoena*; Marino et al., 2003b), the dwarf sperm whale (*Kogia simus*; Marino et al., 2003a), the spinner dolphin (*Stenella longirostris orientalis*; Marino et al., 2004b), and the killer whale (*Orcinus orca*; Marino et al., 2004a). MRI offers a nondestructive method of acquiring a permanent archive of external and internal brain structure data. This technique allows thin virtual sections of the entire brain to be acquired where histological processing is not practical. Furthermore, MRI coupled with advanced software image analysis can accurately determine regional brain volumes (Montie, 2006), while traditional dissection and photography introduces error in performing quantitative measurements. Three-dimensional models of brain structures constructed from MRI scans can also provide a valuable tool to examine spatial relationships among brain structures (Montie, 2006).

MRI can be used also to study the developmental patterns of cetacean brains. In addition, it has great potential as a tool to investigate the impacts of emerging threats on marine mammal health, which include anthropogenic chemicals such as hydroxylated polychlorinated biphenyls (OH-PCBs; Sandala et al., 2004; McKinney et al., 2006) and polybrominated diphenyl ethers (PBDEs; de Boer et al., 1998); land-based pathogen pollution (Conrad et al., 2005); noise pollution (US Department of Commerce, 2001); and biotoxins from harmful algal blooms (HABs; Scholin et al., 2000). These chemical, physical, and biological agents can impact the brain. One example is domoic acid, a type of biotoxin produced by some diatom *Pseudo-nitzschia* species and associated with harmful algal blooms. Domoic acid is neurotoxic and has been shown to cause bilateral hippocampal atrophy in California sea lions (*Zalophus californianus*) (Silvagni et al., 2005). MRI can be used as a diagnostic tool to identify pre- or postmortem brain pathologies associated with such etiologies (Montie, 2006). However, before MRI can be used to diagnose pathologies, an understanding of normal brain structure and changes during development is needed.

Previous neuroanatomical MRI-based atlases of cetaceans were completed on brains that were removed from the skull and formalin fixed (Marino et al., 2001a–c, 2003a,b, 2004a,b). Both the removal and fixation of the brain are factors than can affect the spatial relationships, the integrity, and dimensions of brain structures. Our goal in this study was to present an anatomically labeled MRI-based atlas of the subadult and fetal brain of the Atlantic white-sided dolphin (*Lagenorhynchus acutus*) from MRI scans of fresh, postmortem brains intact, within the skull, with the head still attached to the body. The in situ neuroanatomical MRI-based atlases of the fetal and subadult brains also provided a database for volumetric studies of brain structures in Atlantic white-sided dolphins (Montie et al., 2007).

MATERIALS AND METHODS

Specimens

The subadult specimen (ID#: CCSN05-084-La) used in this study was a male Atlantic white-sided dolphin that stranded live at Wellfleet, Massachusetts, on March 19, 2005. The specimen was humanely euthanized by personnel of the Cape Cod Stranding Network (CCSN) because of injuries related to the stranding. The body length was 156 cm, and the weight was 42.6 kg. The length measurement is consistent with an approximate age of 2–3 years. The specimen was reproductively immature (i.e., immaturity is defined for this species as a length of 141 to 210 cm; Sergeant et al., 1980).

The fetal specimen (ID#: CCSN05-040-La-fetus) used in this study was a male Atlantic white-sided dolphin found in utero in a freshly dead adult female that stranded at Chesequessett Neck, Wellfleet, Massachusetts, on February 15, 2005. The female was transported to the Woods Hole Oceanographic Institution (WHOI) necropsy facility with ice surrounding the head and body cavity. The fetus was removed from the mother within 16 hr of discovery. The body length was 54 cm and the weight was 2.4 kg, consistent with a prenatal stage of 6–9 months (Sergeant et al., 1980). Full gestation period for this species is 11 months with birth lengths of 108 to 122 cm (Sergeant et al., 1980).

Magnetic Resonance Data Acquisition

Both specimens were washed, dried, and placed in transport bags with ice surrounding the head. They were then immediately transported to the MRI facility or temporarily stored in a chiller at 40°F until imaging could be initiated. MRI scanning of the subadult specimen was completed 5 hr postmortem; imaging of the fetus was completed approximately 24 hr postmortem. MRI scanning of the brain in situ were acquired in coronal and sagittal planes with a 1.5-T Siemens Symphony Scanner (Siemens, Munich, Germany) at Shields MRI and CT of Cape Cod, Hyannis, Massachusetts. Two-dimensional proton density (PD) and T2-weighted images were acquired using a fast spin-echo sequence. For the subadult brain, the following parameters were used: TE = 15/106 msec for PD and T2, respectively; TR = 9,000 msec for coronal MRI; TR = 8,000 msec for sagittal MRI; slice thickness = 2 mm; flip angle = 180 degrees; field of view (FOV) = 240 × 240 mm; matrix = 256 × 256; voxel size = 0.9 × 0.9 × 2.0 mm. For fetal brains, the parameters were altered because of the small size of the brain: TE = 15/106 msec for PD and T2, respectively; TR = 8,000 msec; slice thickness = 2 mm; flip angle = 180 degrees; FOV = 200 × 200 mm; matrix = 256 × 256; voxel size = 0.8 × 0.8 × 2.0 mm.

After imaging, the specimens were transported to WHOI and stored at 4°F overnight. A complete necropsy was performed the next day. The brains were carefully removed, weighed, and archived at −80°C.

Image Processing, Volume Analysis, and Three-Dimensional Reconstructions

Visualization was completed first on the MRI unit. Postprocessing, segmentation (i.e., assigning pixels to particular structures), volume analysis, and three-dimensional reconstructions of MRI scans were performed using the software program AMIRA 3.1.1 (Mercury Computer Systems, San Diego, CA). The image processing consisted of the following steps. First, original T2 and PD-weighted DICOM images were corrected for image intensity nonuniformity by applying a Gaussian filter. The processed results were then subtracted from the original images to generate a "filtered" image set. The new image set was rotated and realigned in the coronal plane to correct for head tilt and/or differences in head position. From this "filtered and realigned" data set, a brain surface mask was produced to determine edges for digital removal of nearby blubber, muscle, skull, and other head anatomy. The mask was constructed by manually tracing the surface of the brain and deleting all pixels outside this trace for each MRI scan. These resulting images are referred to as the "processed" PD and T2 images (vs. the original "native" PD and T2 images).

Total brain volumes for the subadult and fetus were calculated by integrating the area of each slice of the brain surface mask derived from the coronal "processed" PD images. The caudal boundary of the brain was defined as the termination of the spinal cord at the posterior aspect of the foramen. Virtual brain weight was calculated by multiplying the total brain segmented volume by the assumed specific gravity of brain tissue, 1.036 g/cm^3 (Stephan et al., 1981). Three-dimensional reconstructions of the entire brain were constructed from the segmentation of the brain surface mask that was derived from the coronal "processed" PD images.

Anatomic Labeling and Nomenclature

One disadvantage of image processing is a potential loss of resolution (Evans et al., 2006). For this reason, the two-dimensional images in this atlas of the subadult and fetal brains used "native" images. Anatomical structures were identified and labeled in coronal and sagittal MRI scans of the subadult and the fetus brains. In the subadult, native PD-weighted images were used in the labeled schematics, because these images had better detail of structure edges than the corresponding T2-weighted images. For the labeled illustrations of the fetus, native T2-weighted images were used, because these images displayed better detail of structure edges than PD-weighted images, which was most likely a function of higher water content in fetal brains (Almajeed et al., 2004). Anatomical nomenclature was adopted from Morgane et al. (1980). MRI scans of the subadult and fetal brains in this study were also compared with previous findings of the bottlenose dolphin and of the fetal common dolphin (Marino et al., 2001b,c).

RESULTS AND DISCUSSION

Volume Estimates of the Entire Brain

Segmentations of processed PD-weighted images were used to delineate the brain surface and calculate the total brain volumes. Calculated volumes of the entire brain were 1,019.4 cm^3 for the subadult and 127.9 cm^3 for the fetus. Three-dimensional reconstructions of these volumes were constructed from the MRI scans (Fig. 1). The virtual brain weights (calculated by multiplying the measured volume by the specific gravity of brain tissue) were 1,056.1 g for the subadult and 132.5 g for the fetus. These estimates were very similar to the actual measured extracted brain weights (i.e., 1,057.8 g for the subadult and 131.9 g for the fetus).

Three-Dimensional Reconstructions and Neuroanatomy of the Subadult Brain

Three-dimensional reconstructions of the brain from MRI scans of the subadult displayed the classic hallmarks of odontocete brains, as described in previous studies (Marino et al., 2001a–c, 2003a,b, 2004a,b; Fig. 1). The most striking feature was the foreshortened frontal lobes and the pronounced temporal width, with no olfactory structures in the frontal lobe region. This gave the brain "a boxing glove" appearance typical of odontocetes that was first reported by Morgane et al. (1980). This brain shape is different from that of other mammals and may result from evolutionary changes that occurred during telescoping of the skull (Morgane et al., 1980; Marino et al., 2001a). On the other hand, it is also possible that the brain changed shape because olfactory structures were lost and acoustic structures were enlarged (Morgane et al., 1980; Marino et al., 2001a).

Figures 2–9 display an anterior-to-posterior sequence of PD native, 2.0-mm-thick coronal MRI brain sections at 10-mm intervals. Panels A illustrate the position of the brain in the coronal plane relative to surrounding head structures of the native PD image; panels B show labeled schematics of each brain section removed from the head structure with the conventional MRI gray scale inverted (i.e., white matter appears white and cerebrospinal fluid [CSF] appears black); panels C display a sagittal section showing the orientation and level at which the native PD section was taken.

Figures 10–17 display a midline-to-lateral sequence of native PD, 2.0-mm-thick sagittal MRI brain sections at 10-mm intervals through the left hemisphere. Panels A illustrate the position of the brain in the sagittal plane relative to surrounding head structures of the native PD image; panels B show labeled images of each brain section excised from the head structure with the conventional MRI gray scale inverted; panels C display a coronal section showing the orientation and level at which the native PD section was taken. These figures illustrate undisturbed spatial relationships among brain structures and surrounding head anatomy obtainable by MRI scanning of fresh, intact postmortem heads.

Telencephalon. The MRI scans showed distinguishing features of the odontocete telencephalon. The neocortex is highly convoluted (Figs. 2B–17B). The limbic and paralimbic clefts, which divide the limbic, paralimbic, and supralimbic lobes, were visible (Figs. 2B–

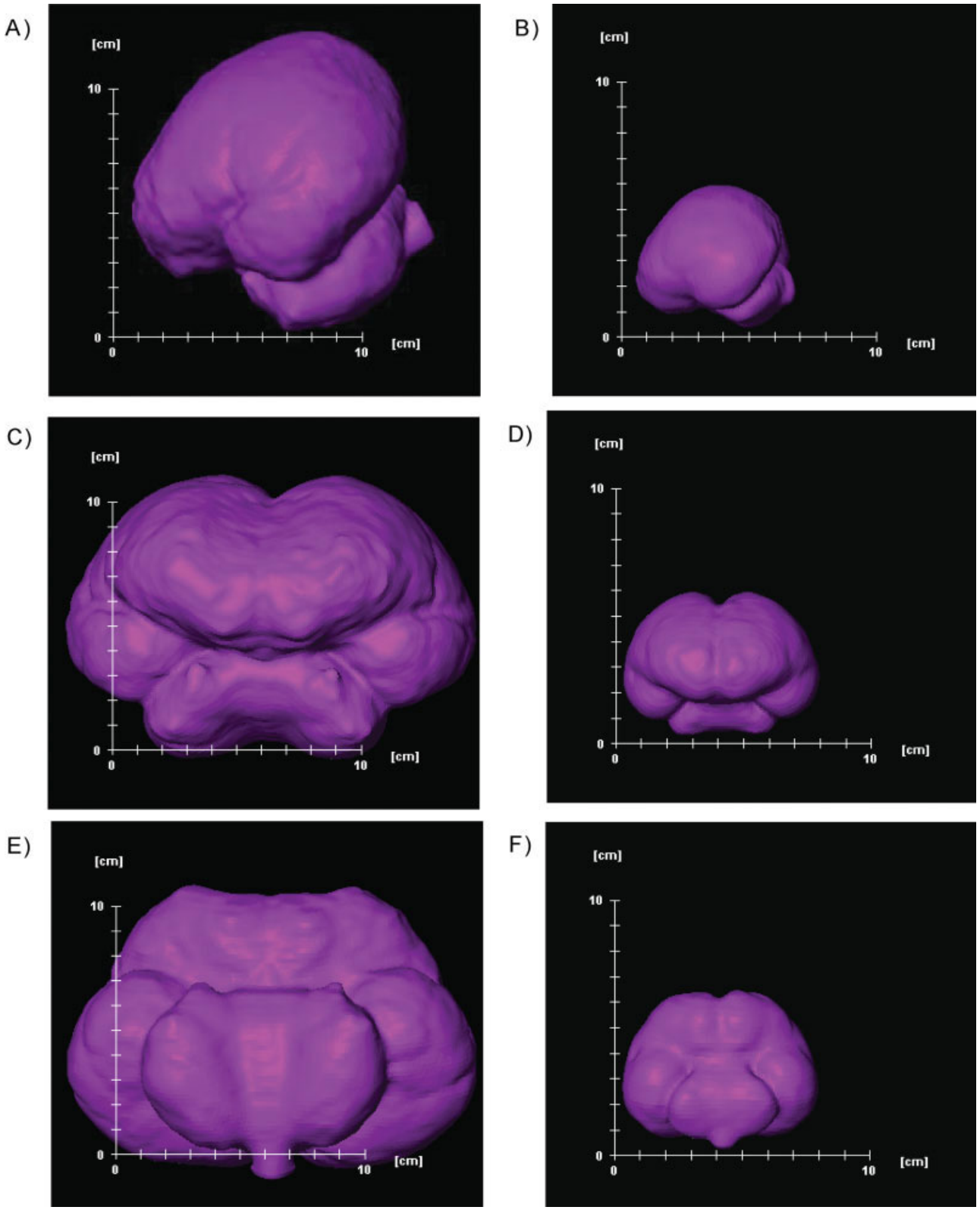

Figure 1. Three-dimensional reconstructions of the subadult and fetal brain from magnetic resonance images. **A:** Left view of subadult brain. **B:** Left view of fetal brain. **C:** Anterior view of subadult brain. **D:** Anterior view of fetal brain. **E:** Ventral view of subadult brain. **F:** Ventral view of fetal brain.

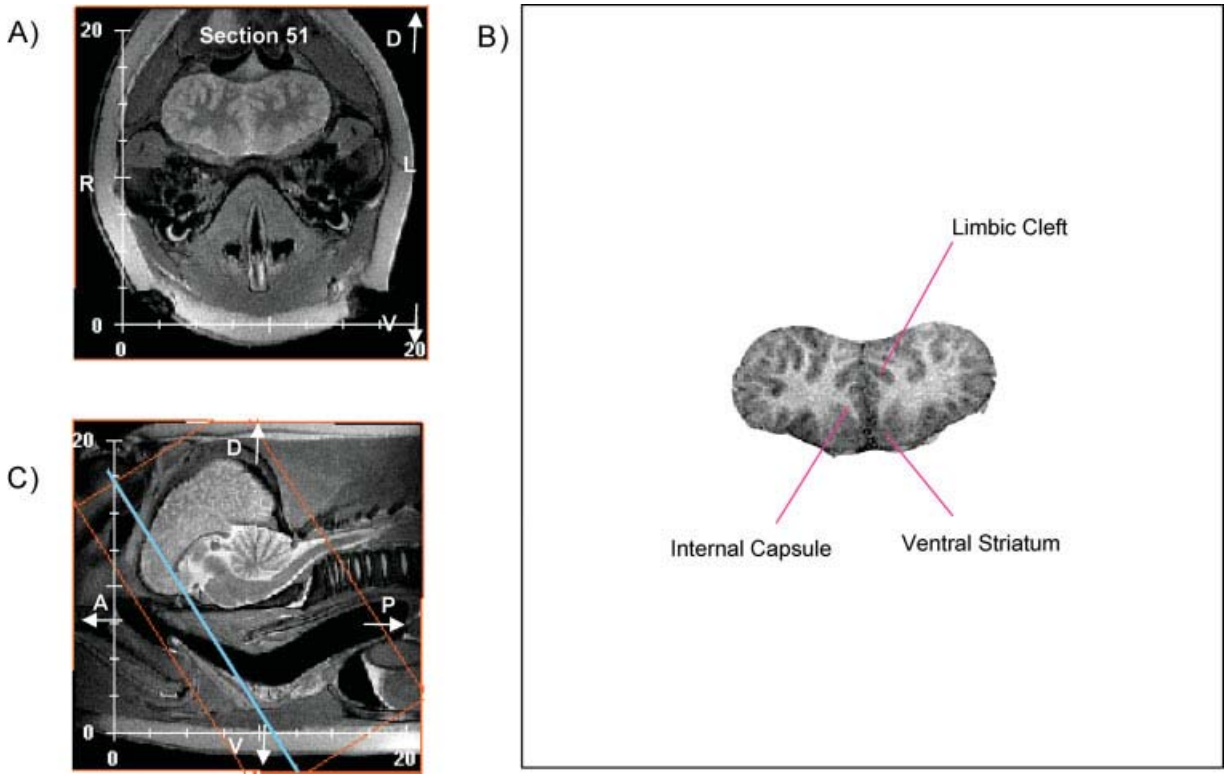

Figure 2. (Legend on page 1466)

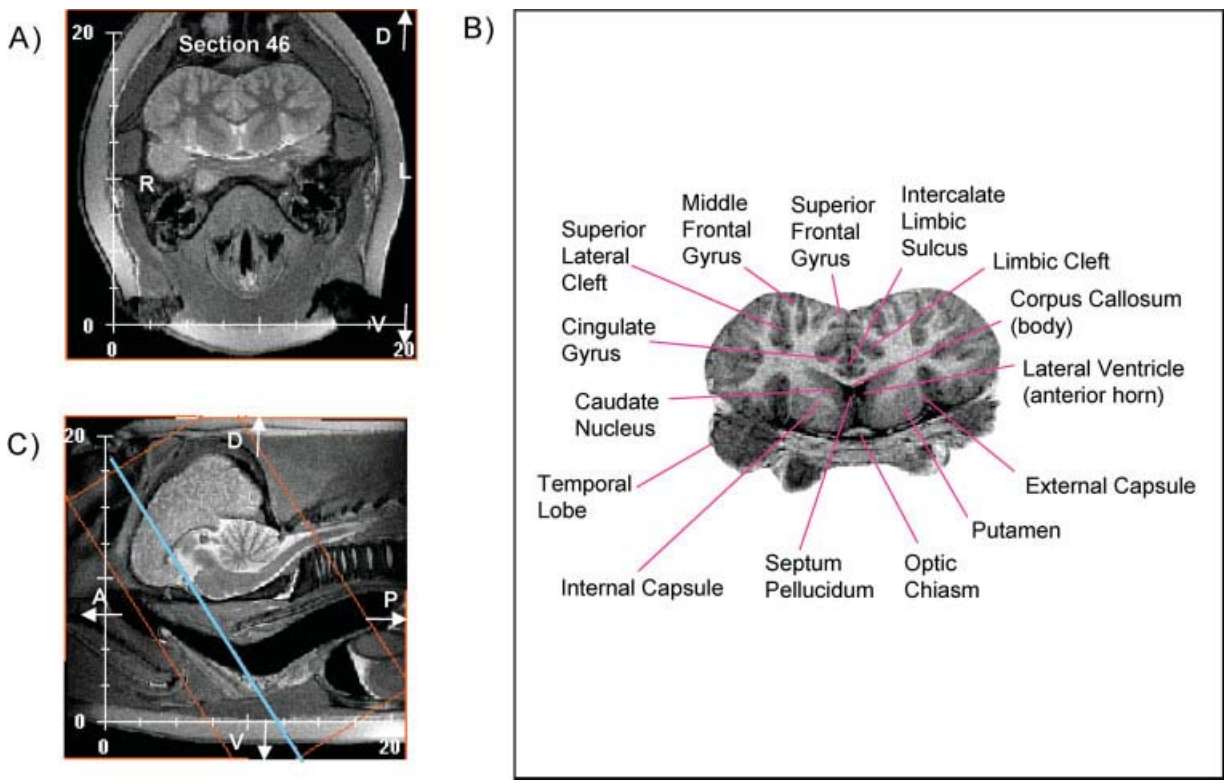

Figure 3. (Legend on page 1466)

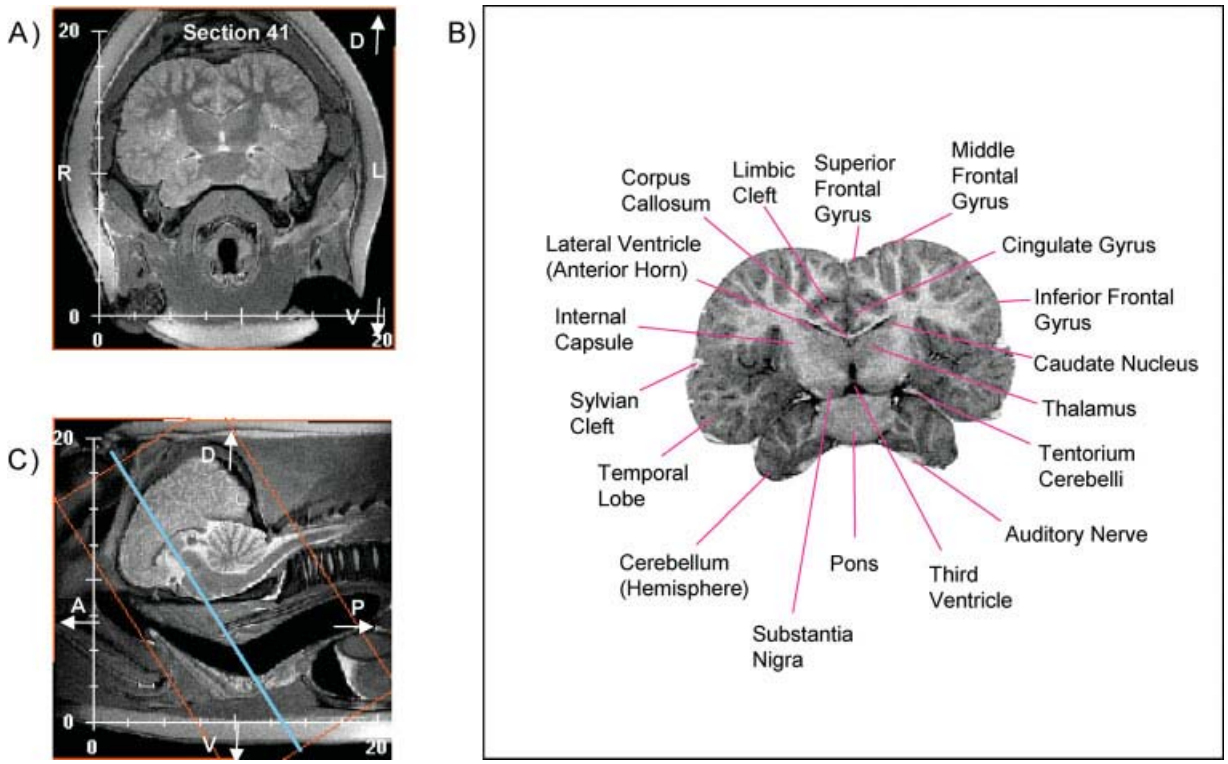

Figure 4. (Legend on page 1466)

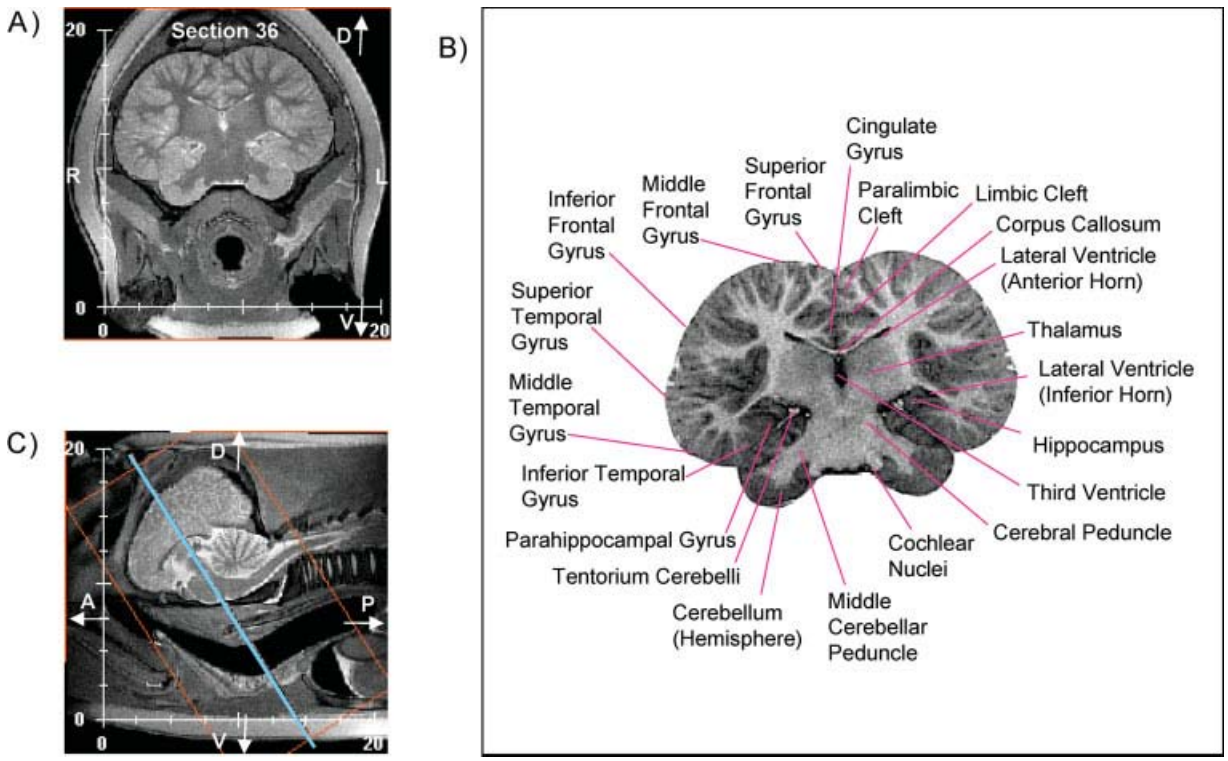

Figure 5. (Legend on page 1466)

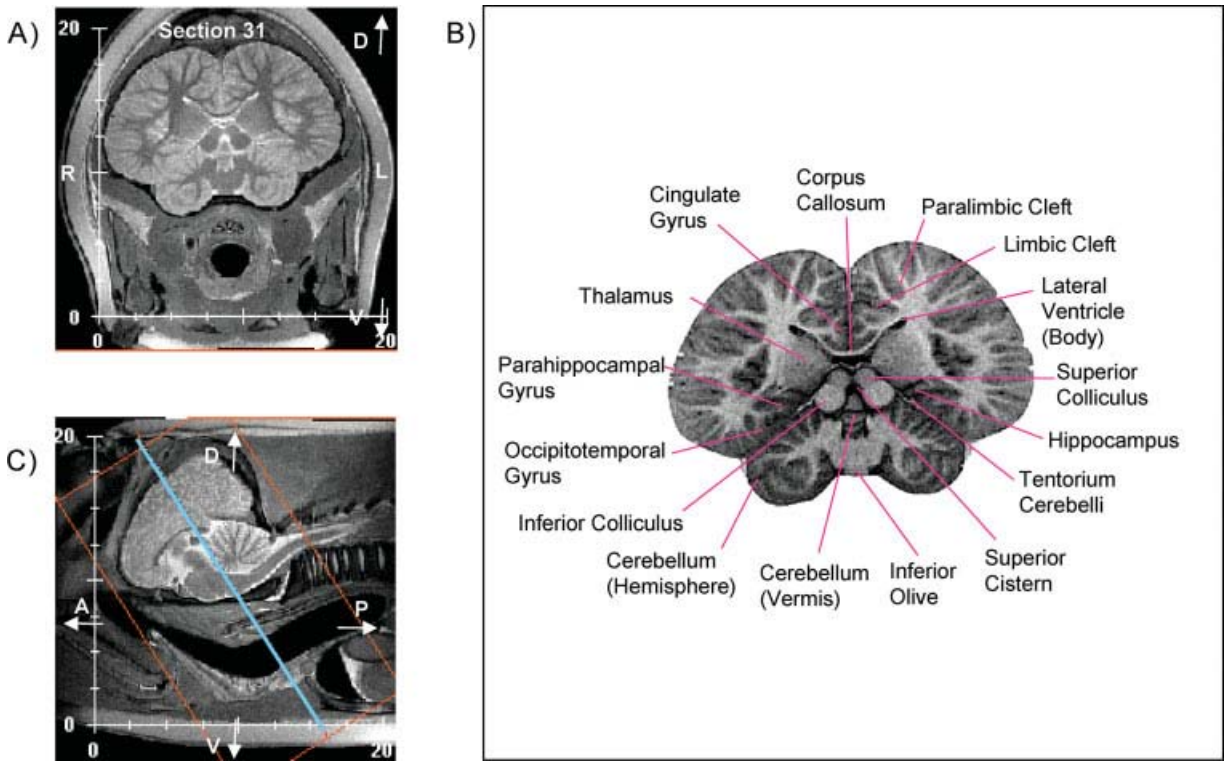

Figure 6. (Legend on page 1466)

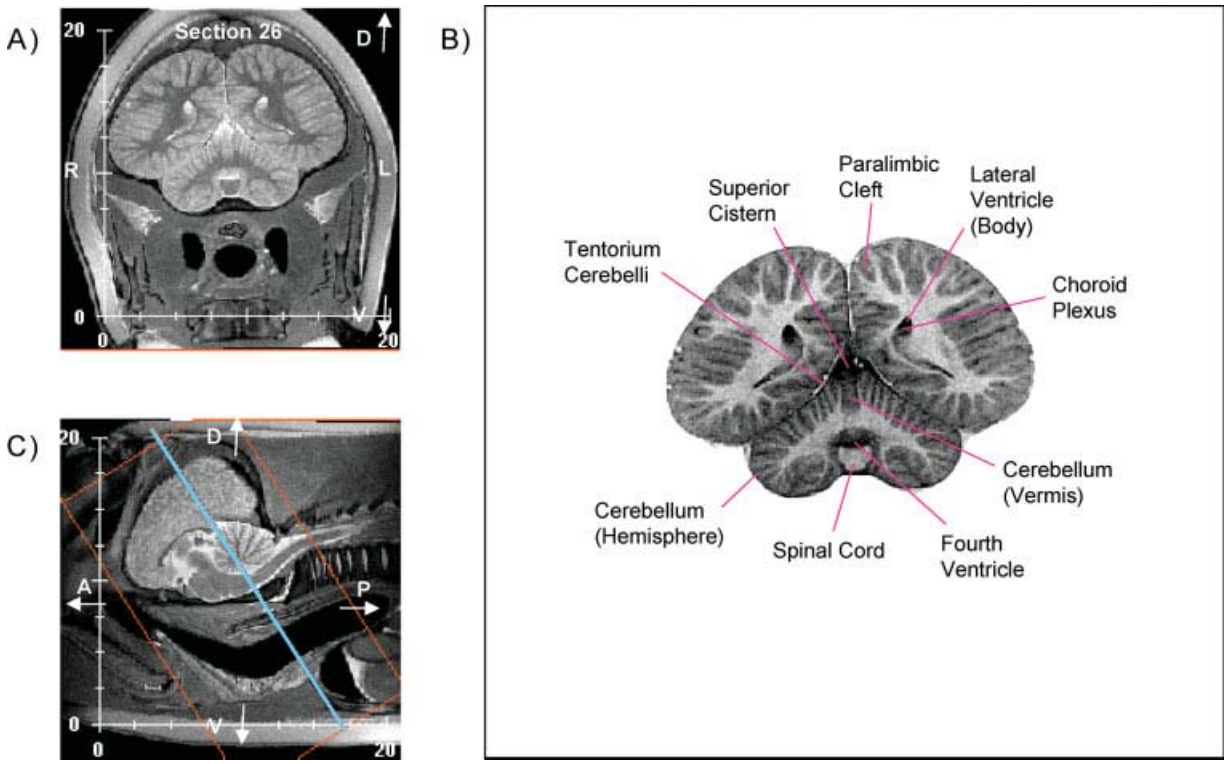

Figure 7. (Legend on page 1466)

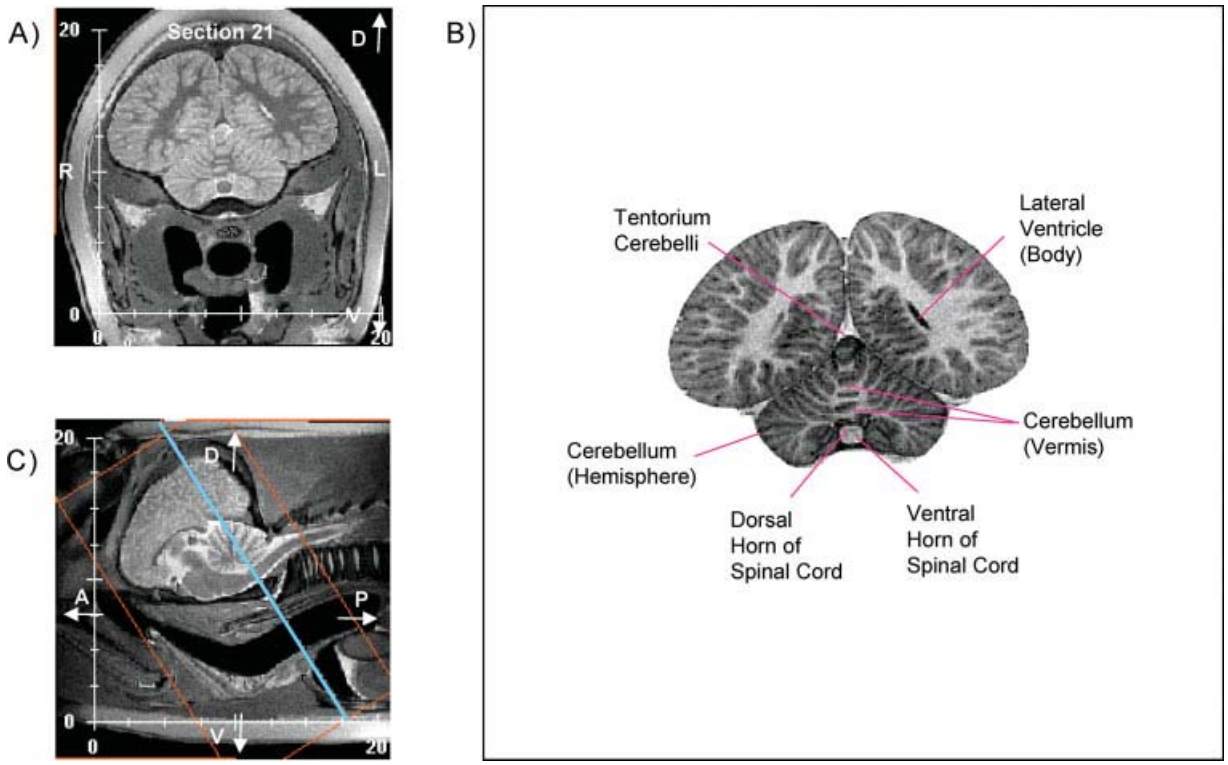

Figure 8.

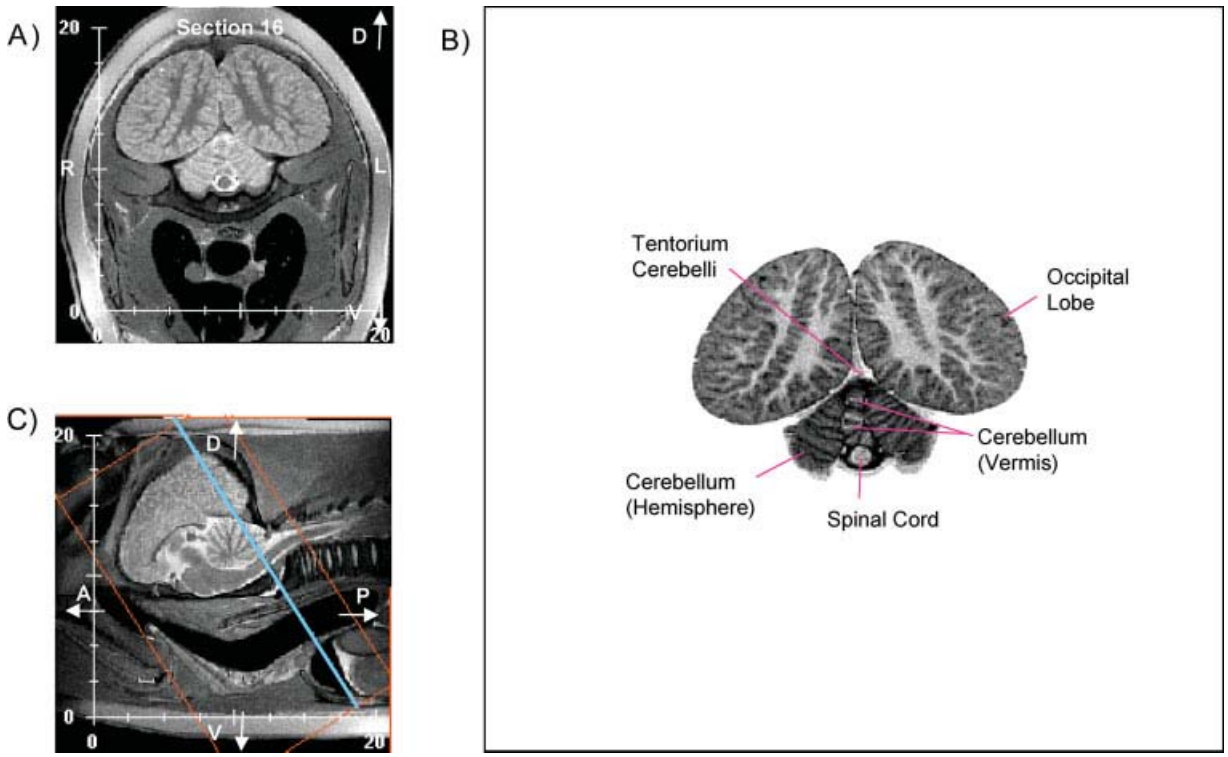

Figure 9.

Figures 2–9. Anterior-to-posterior sequence of coronal in situ magnetic resonance imaging (MRI) scans of the subadult brain. **A:** Native proton density (PD) -weighted 2.0-mm-thick coronal MRI brain sections at 10-mm intervals. **B:** Labeled brain removed from the head structure with the conventional MRI gray scale inverted. White matter appears white; gray matter appears gray; and cerebrospinal fluid appears black. **C:** Sagittal MRI scans of the brain intact within the skull depicting the orientation of the section. Orange lines illustrate the span of the MRI sequence. Blue lines represent the plane of section. D, dorsal; V, ventral; L, left; R, right; A, anterior; P, posterior. Scale is in cm.

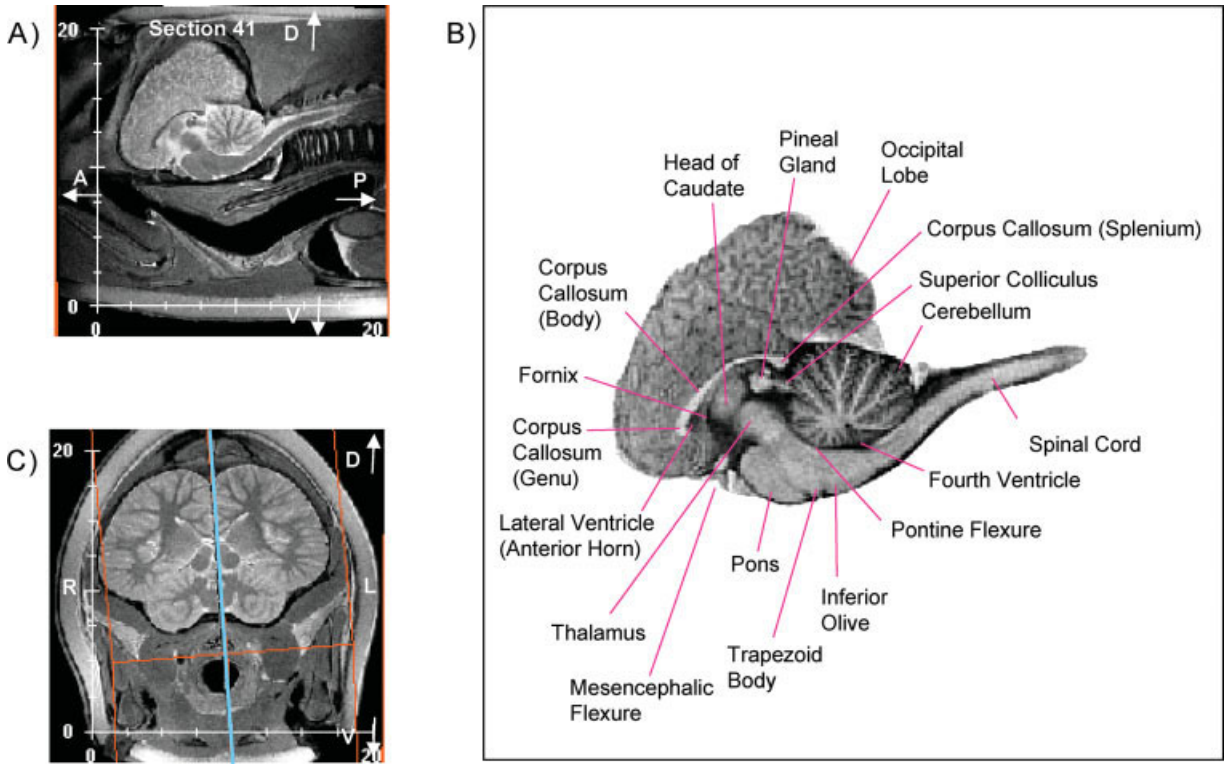

Figure 10. (Legend on page 1470)

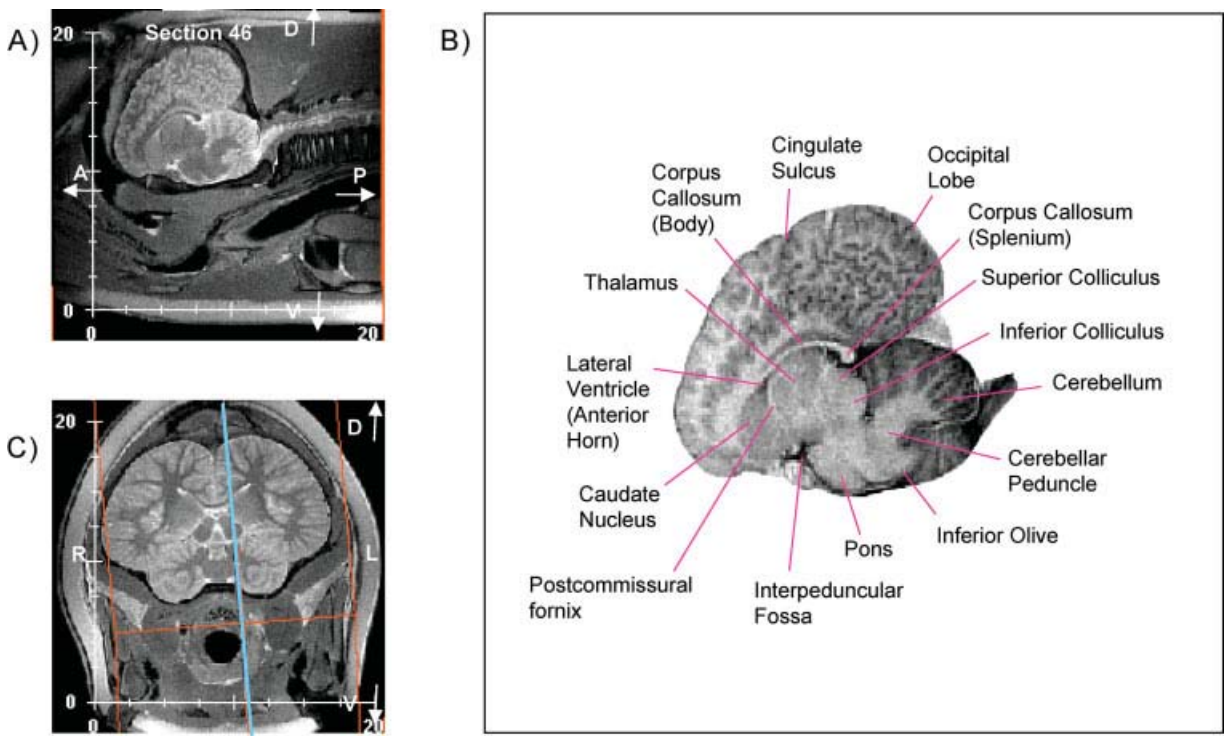

Figure 11. (Legend on page 1470)

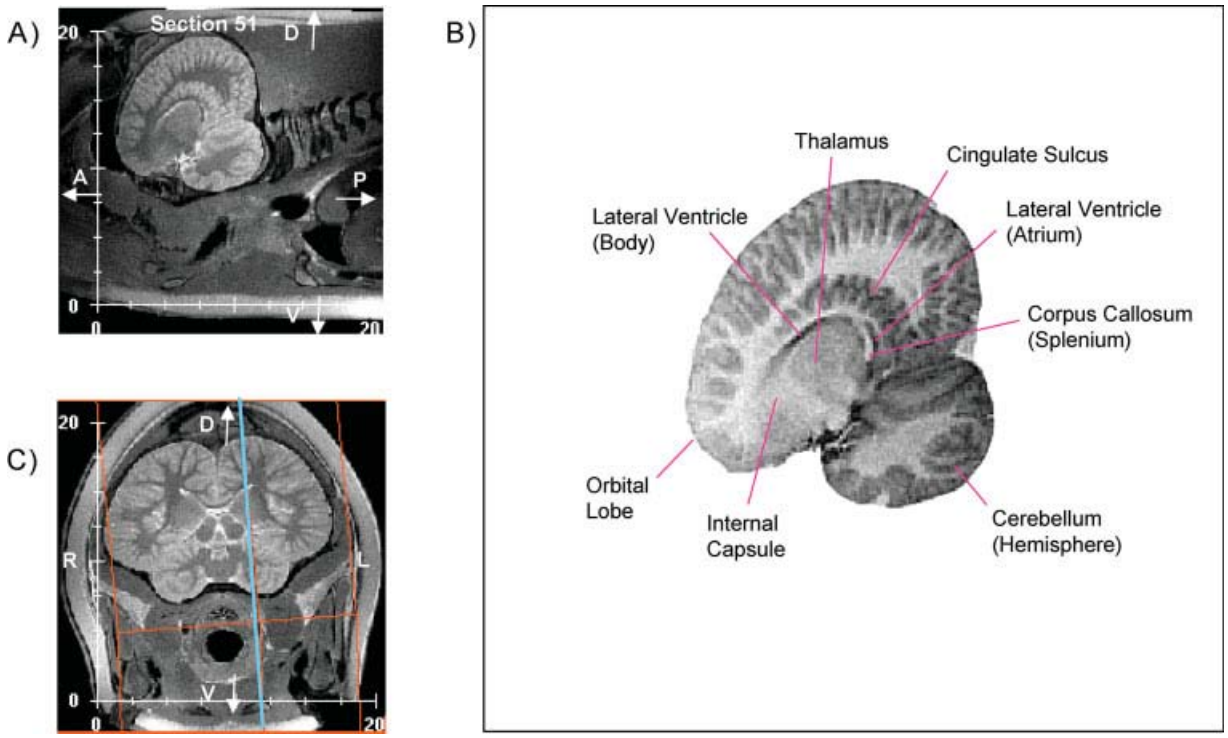

Figure 12. (Legend on page 1470)

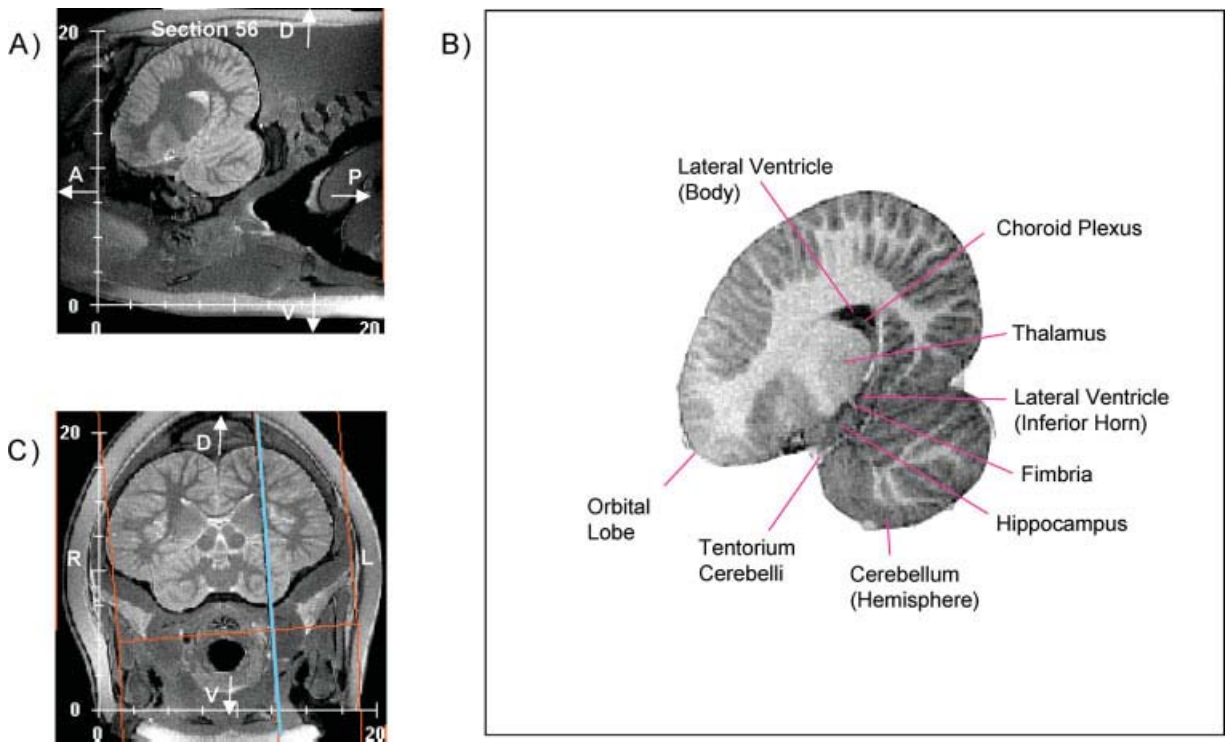

Figure 13. (Legend on page 1470)

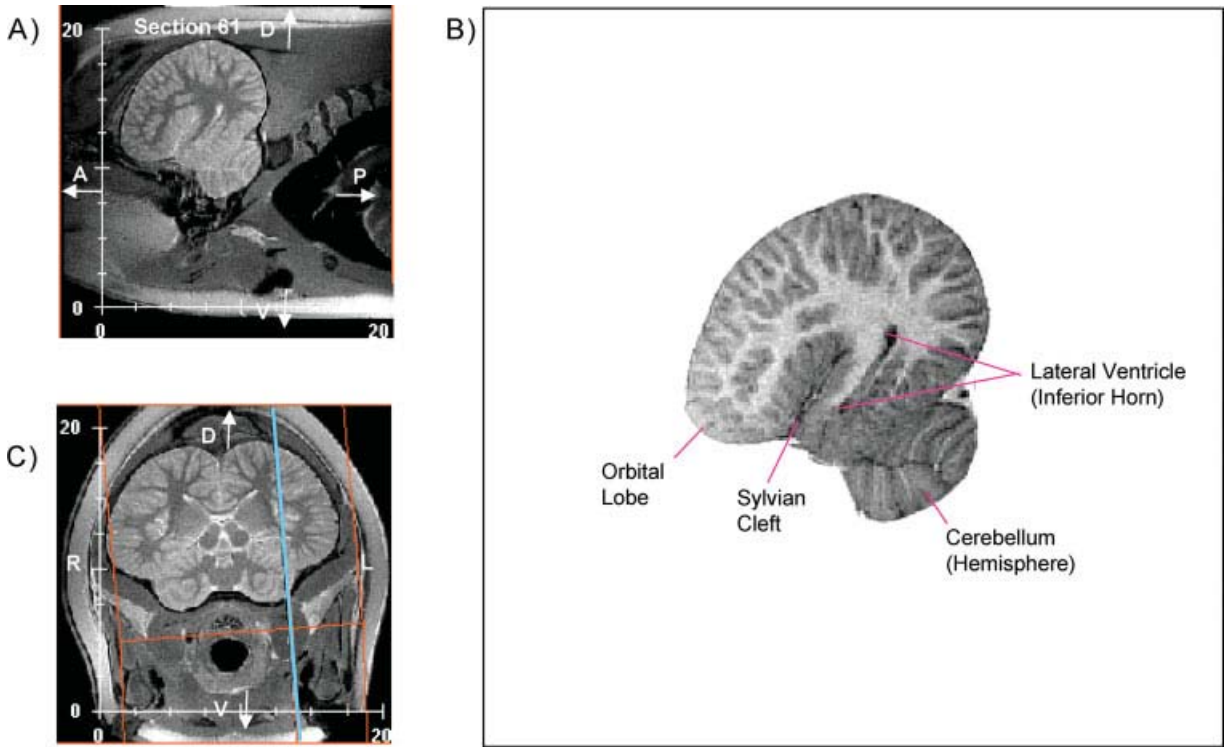

Figure 14. (Legend on page 1470)

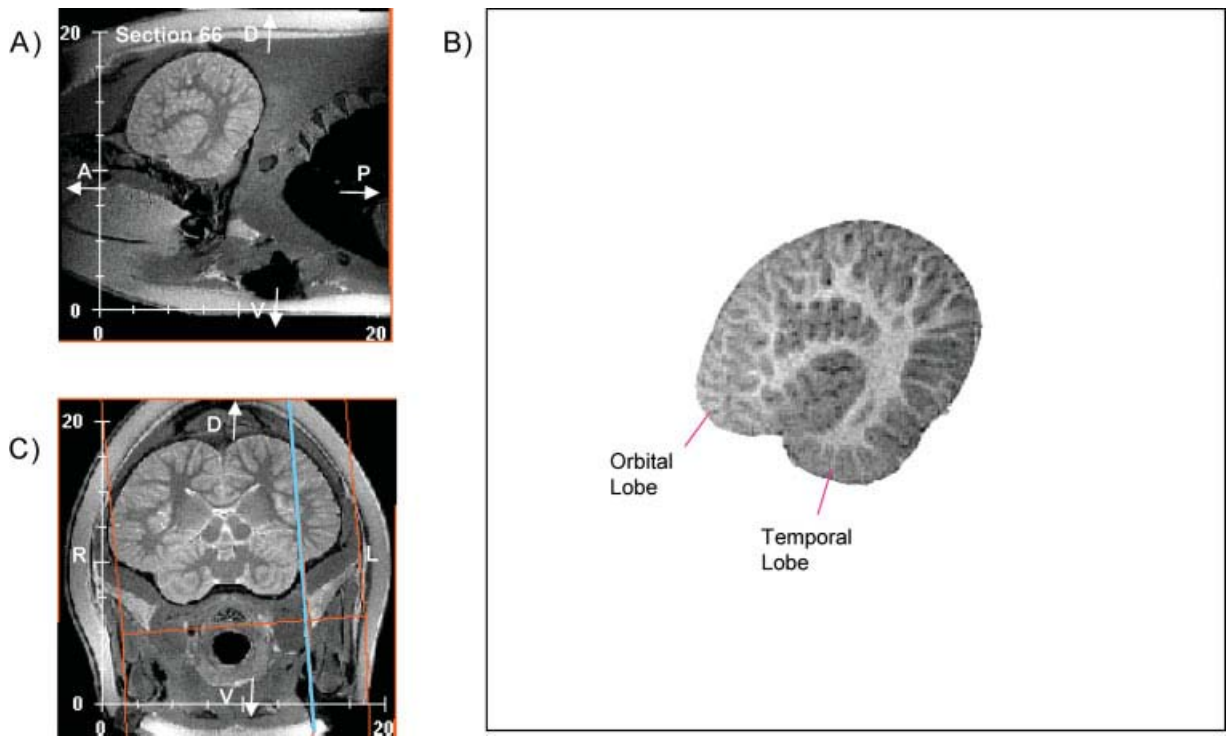

Figure 15. (Legend on page 1470)

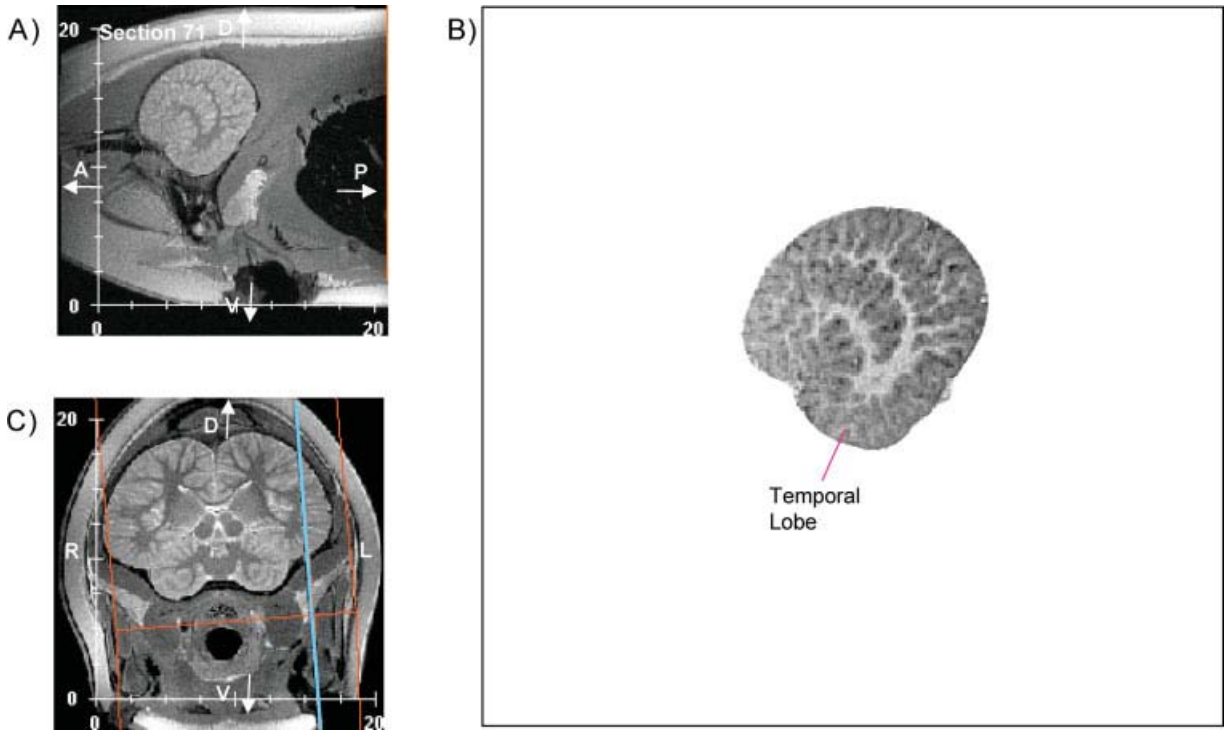

Figure 16.

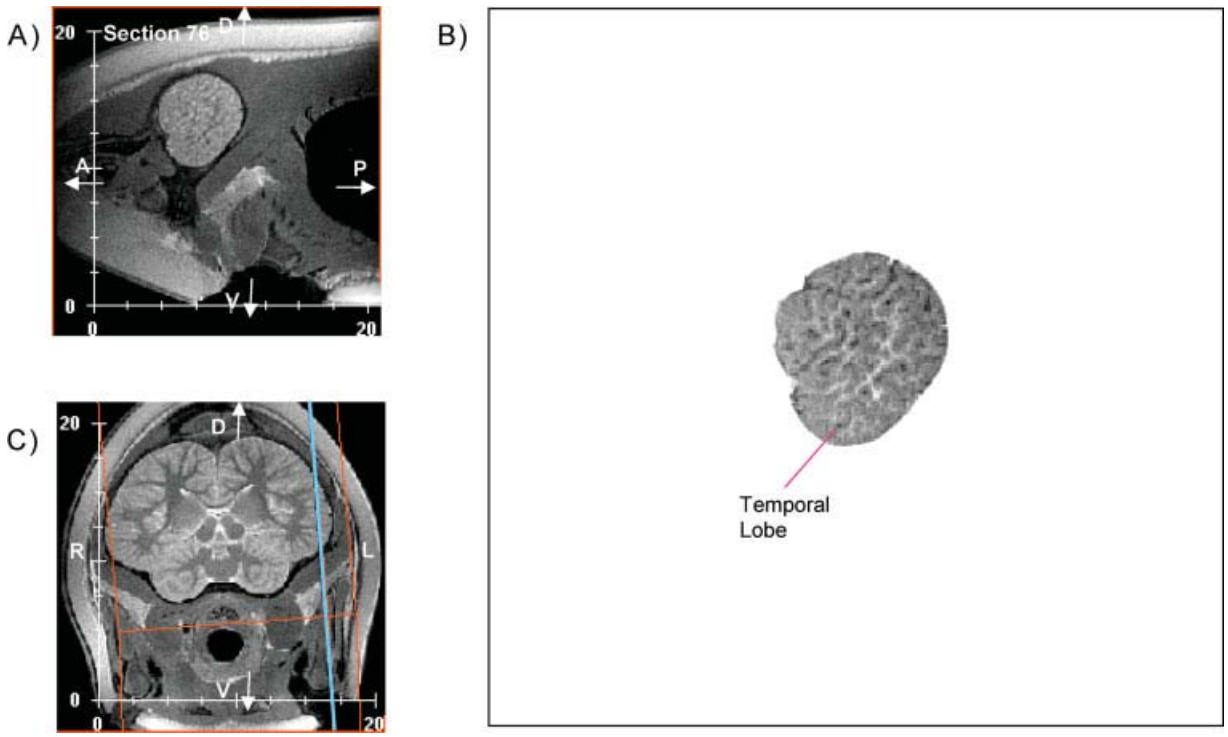

Figure 17.

Figures 10–17. Midline-to-lateral sequence of sagittal in situ magnetic resonance imaging (MRI) scans of the subadult brain. **A:** Native proton density (PD) -weighted 2.0-mm-thick sagittal MRI brain sections of the left hemisphere at 10-mm intervals. **B:** Labeled brain excised from the head structure with the conventional MRI gray scale inverted. White matter appears white; gray matter appears gray; and cerebrospinal fluid appears black. **C:** Coronal MRI scans of the brain intact within the skull depicting the orientation of the section. Orange lines illustrate the span of the MRI sequence. Blue lines represent the plane of section. D, dorsal; V, ventral; L, left; R, right; A, anterior; P, posterior. Scale is in cm.

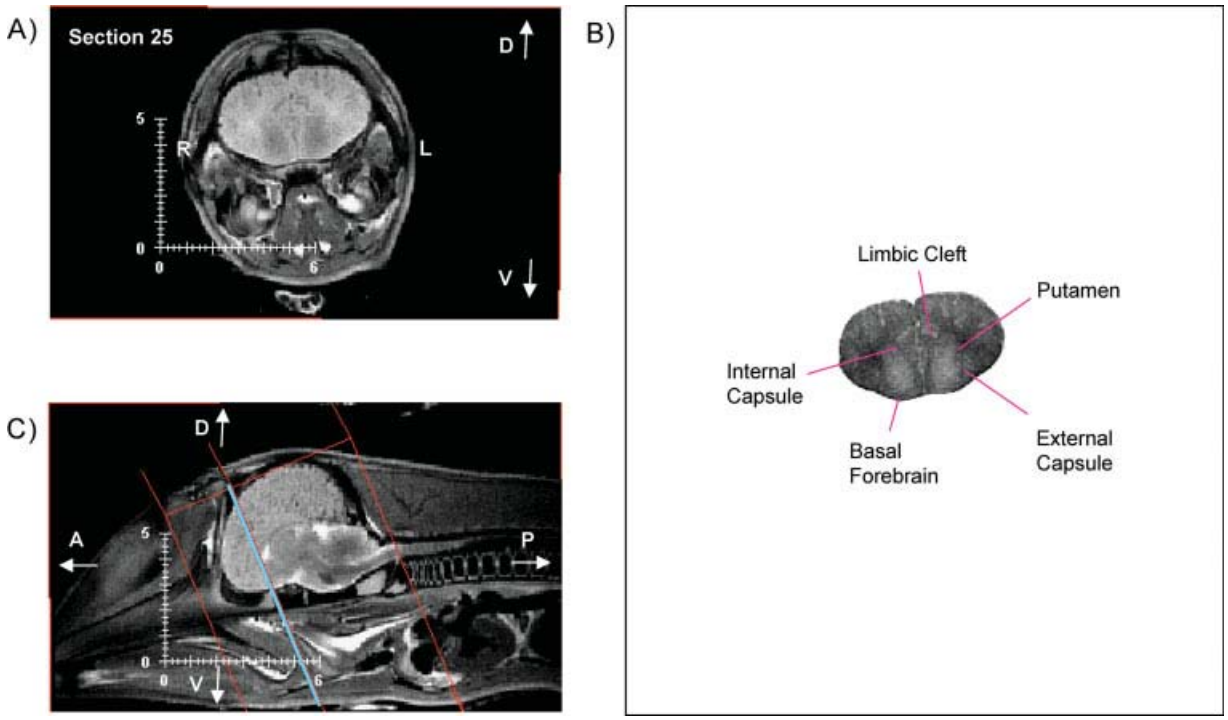

Figure 18. (Legend on page 1474)

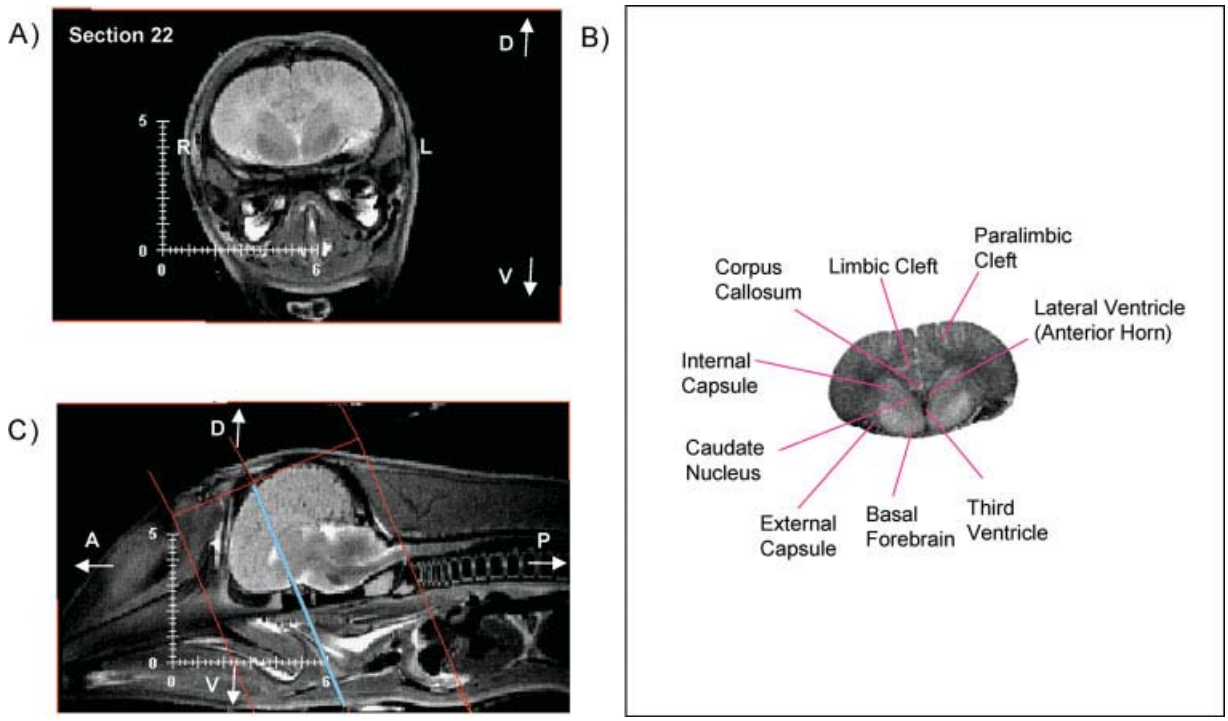

Figure 19. (Legend on page 1474)

7B). Structures of the basal ganglia (such as the caudate nucleus and the putamen) were recognized (Figs. 2B–4B, 11B). Unlike previous reports of MRI studies of formalin-fixed brains in small delphinids (Marino et al., 2001b,c, 2004b), the hippocampus was evident; it was quite small relative to the overall size of the brain and temporal lobes in particular (Figs. 5B–6B; 13B). This observation was similar to the

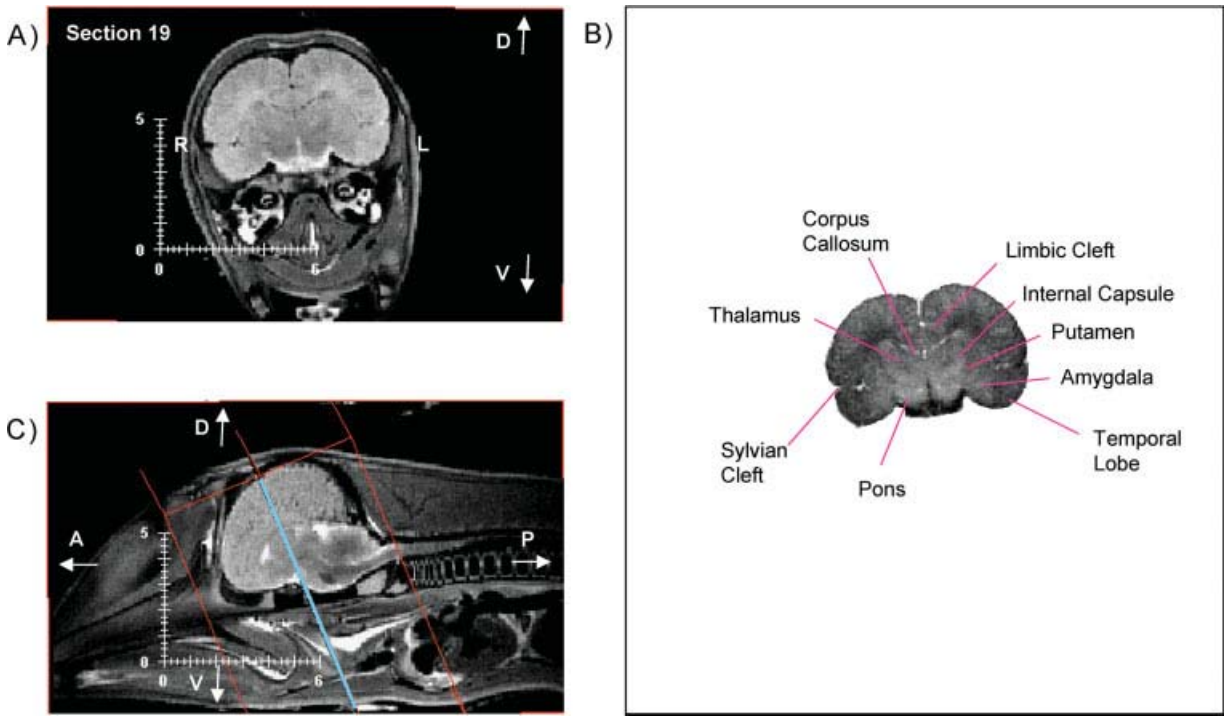

Figure 20. (Legend on page 1474)

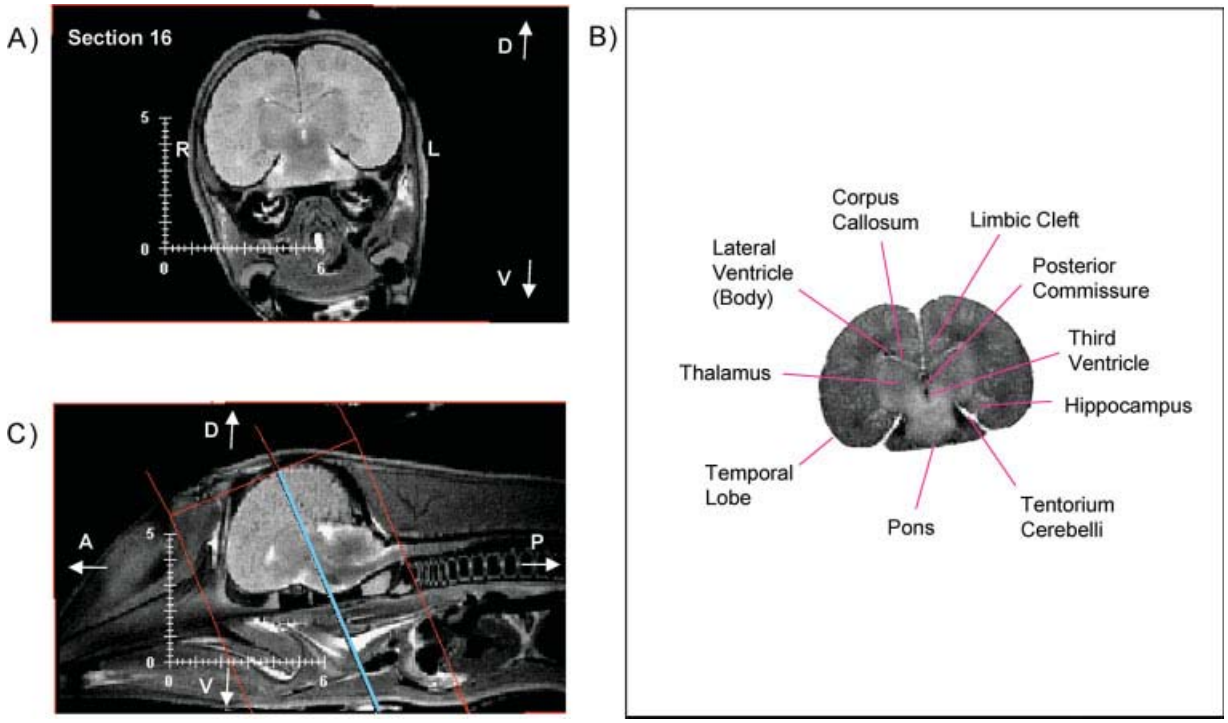

Figure 21. (Legend on page 1474)

findings on the bottlenose dolphin hippocampus by Jacobs et al. (1979). The hippocampus was located more central in the medial wall of the temporal lobes. The boundaries of the hippocampus were best observed in native T2-weighted images rather than the PD-weighted images. This finding can be best explained by the CSF surrounding the hippocampus, as observed by the hyperintensity of the inferior horn of the lat-

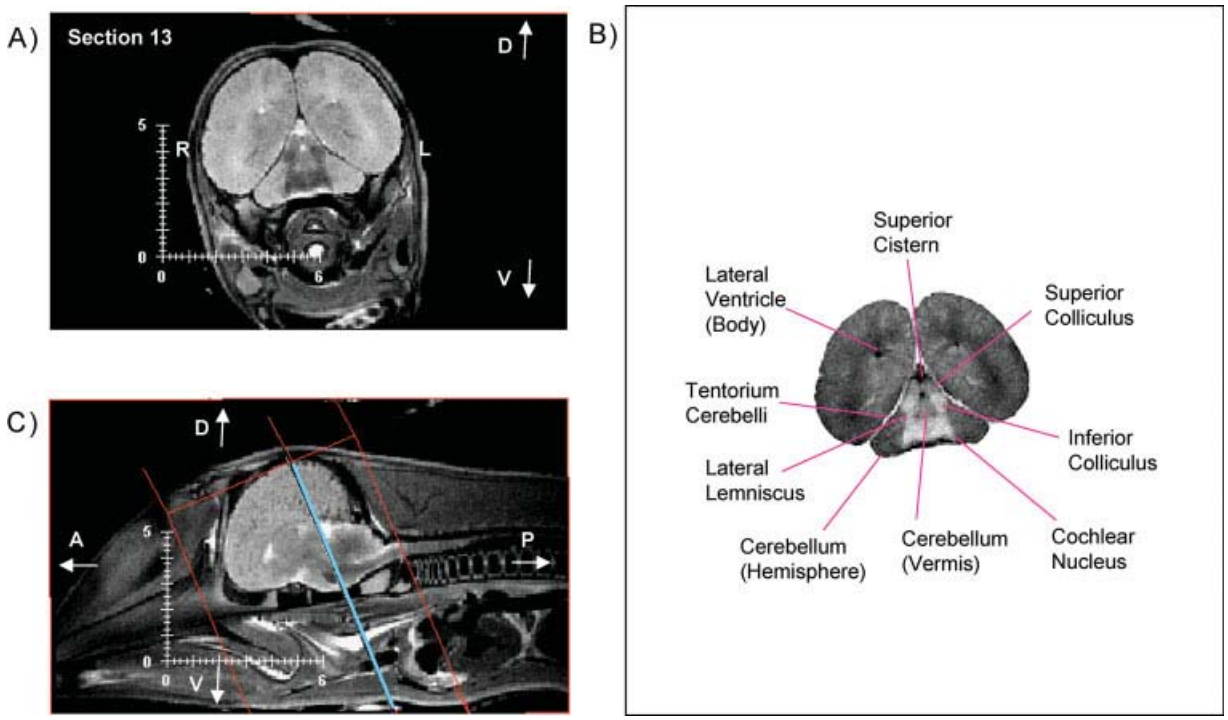

Figure 22. (Legend on page 1474)

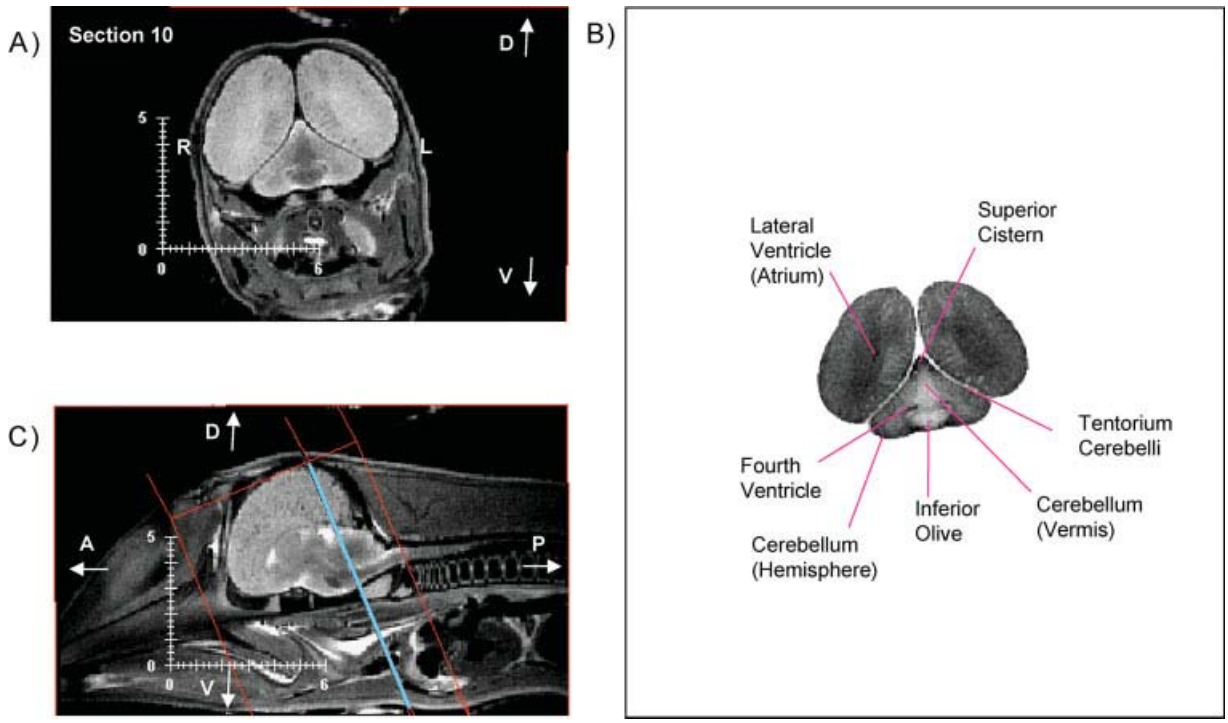

Figure 23. (Legend on page 1474)

eral ventricle (lateral border), the hyperintensity of the parahippocampal sulcus (ventral border), and the hyperintensity of the subarachnoid space (the medial and dorsal borders).

Despite the large hemispheres, the corpus callosum is comparatively small (Figs. 3B–6B, 10B–12B). This is similar to previous findings in other odontocete species (Tarpley and Ridgway, 1994).

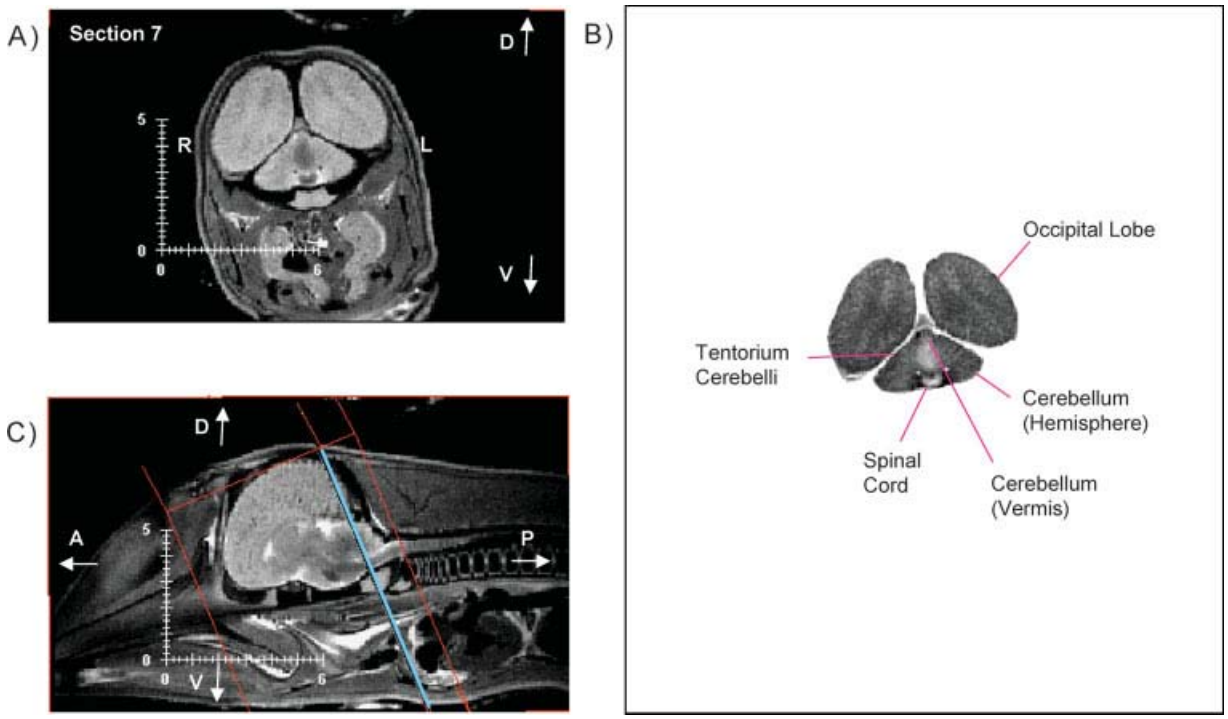

Figure 24.

Figures 18–24. Anterior-to-posterior sequence of coronal in situ magnetic resonance imaging (MRI) scans of the fetal brain. **A:** Native T2-weighted 2.0-mm-thick coronal MRI brain sections at 6-mm intervals. **B:** Labeled brain removed from the head structure with the conventional MRI gray scale inverted. White matter appears white; gray matter appears gray; and cerebrospinal fluid appears black. **C:** Sagittal MRI scans of the brain intact within the skull depicting the orientation of the section. Orange lines illustrate the span of the MRI sequence. Blue lines represent the plane of section. D, dorsal; V, ventral; L, left; R, right; A, anterior; P, posterior. Scale is in cm.

Diencephalon. The MRI scans revealed a large diencephalon in the Atlantic white-sided dolphin. The thalamus was easily recognized and is massive (Figs. 4B–6B, 10B–13B), as expected from the size of the hemispheres.

Mesencephalon. The MRI scans of the subadult Atlantic white-sided dolphin brain illustrate the enlargement of auditory processing regions in odontocete brains. The inferior colliculus is much larger than the superior colliculus (Figs. 6B, 11B).

Metencephalon and Myelencephalon. The MRI scans showed typical characteristics of the odontocete metencephalon and myelencephalon. Auditory pathways were easily observed, including the large auditory nerve (Fig. 4B) and the cochlear nuclei (Fig. 5B). The cerebellum is large, and the white matter and gray matter are easily distinguishable (Figs. 4B–9B, 10B–14B). The large cerebellum in Atlantic white-sided dolphins noted in this study is similar to previous findings in other delphinid species (Ridgway, 1990; Marino et al., 2001c, 2004b). Hindbrain structures including the pons and inferior olive as well as the spinal cord (including the dorsal and ventral horns) were identified (Figs. 4B–9B, 10B–11B).

Three-Dimensional Reconstructions and Neuroanatomy of the Fetal Brain

Three-dimensional reconstructions of the fetal brain from MRI scans also revealed distinguishing characteristics of odontocete brains (Fig. 1). This brain already had adult shape (i.e., foreshortened frontal lobes and the pronounced width) with a "boxing glove" appearance. No olfactory structures were observed in the frontal lobe of this embryo, in contrast to previous MRI findings of a common dolphin fetal brain (Marino et al., 2001b). The mesencephalic and pontine flexures were identifiable.

Magnetic resonance images of the fetus revealed interesting features of neurodevelopment in odontocete brains (Figs. 18–30), similar to those described by Marino et al. (2001b). Figures 18–24 display an anterior-to-posterior sequence of T2 native, 2.0-mm-thick coronal MRI brain sections at 6-mm intervals. Figures 25–30 display a midline-to-lateral sequence of native T2, 2.0-mm-thick sagittal MRI brain sections at 6-mm intervals through the left hemisphere. The figures (panels A, B, and C) were organized similarly to the MRI scans of the subadult. These figures also illustrate the preservation of spatial relationships among brain structures and surrounding head anatomy that is gained from in situ MRI scanning of fresh postmortem fetal brains.

Telencephalon. The MRI scans of the telencephalon showed hallmarks of fetal brains in general and of odontocetes in particular. The native T2 images illustrate the lack of myelinated white matter tracts (light in native T2 images; dark in inverted images) in the telencephalon this early in development (Figs. 18B–24B, 26B–29B) compared with the subadult brain (Figs. 2B–9B, 11B–16B). Structures of the basal ganglia (such as

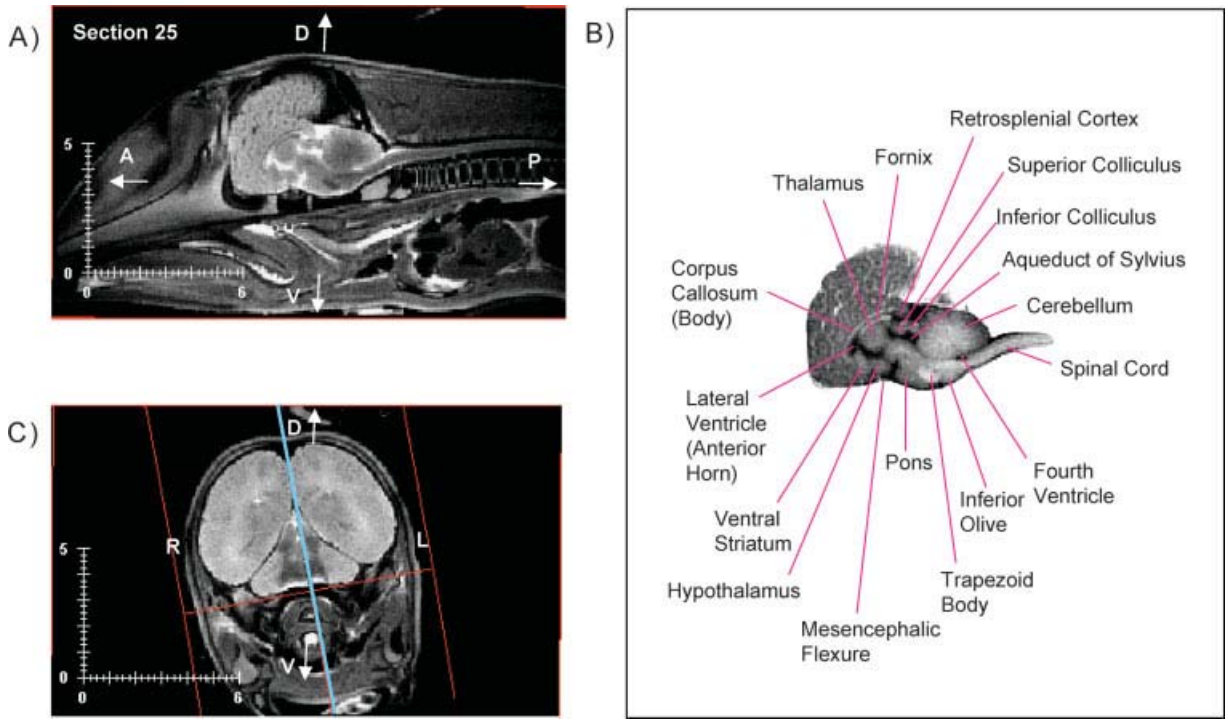

Figure 25. (Legend on page 1477)

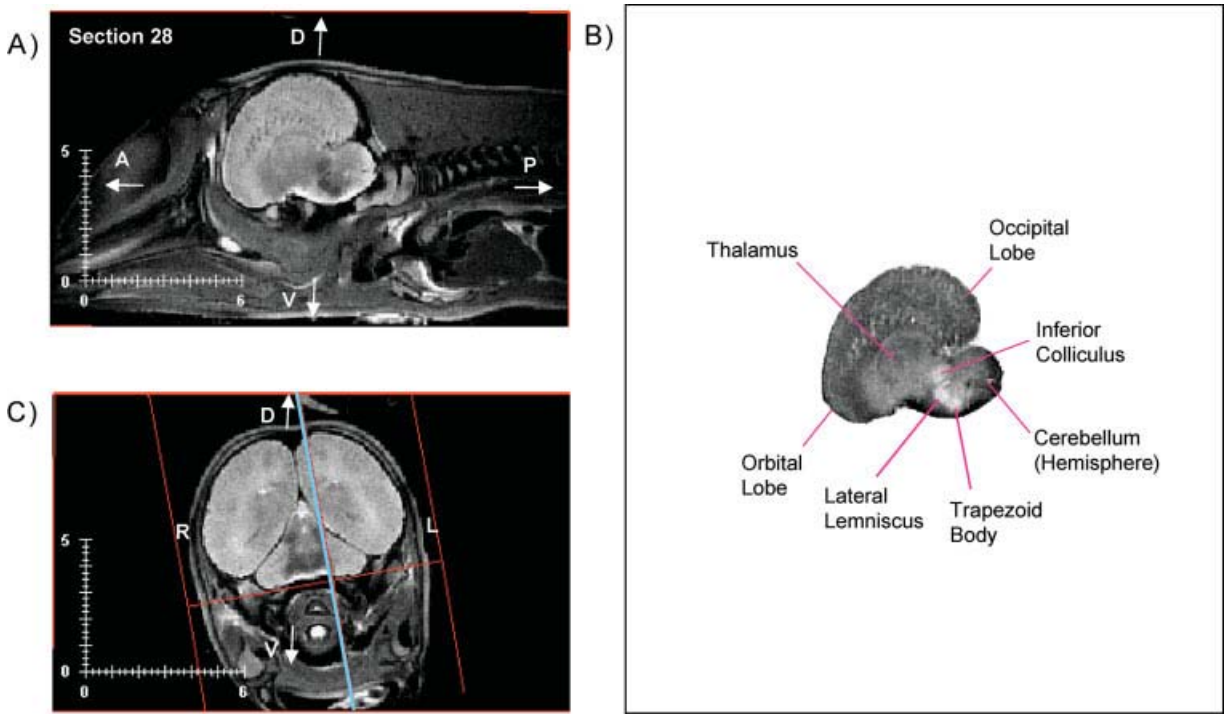

Figure 26. (Legend on page 1477)

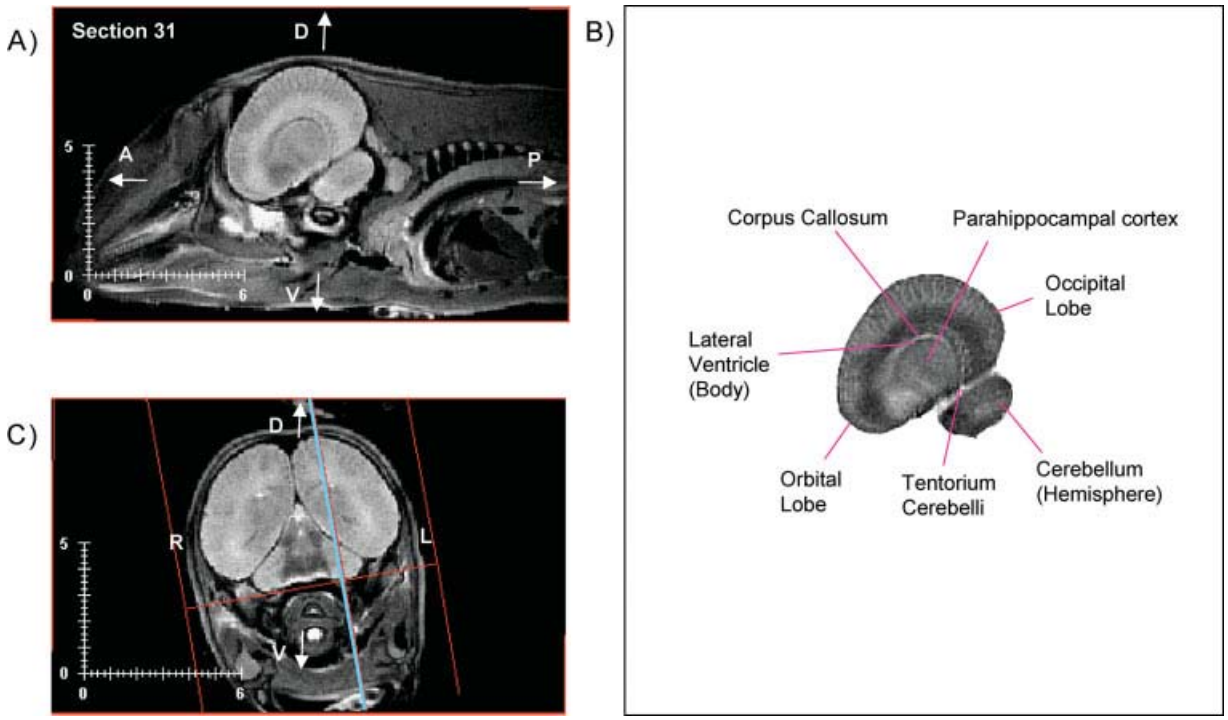

Figure 27. (Legend on page 1477)

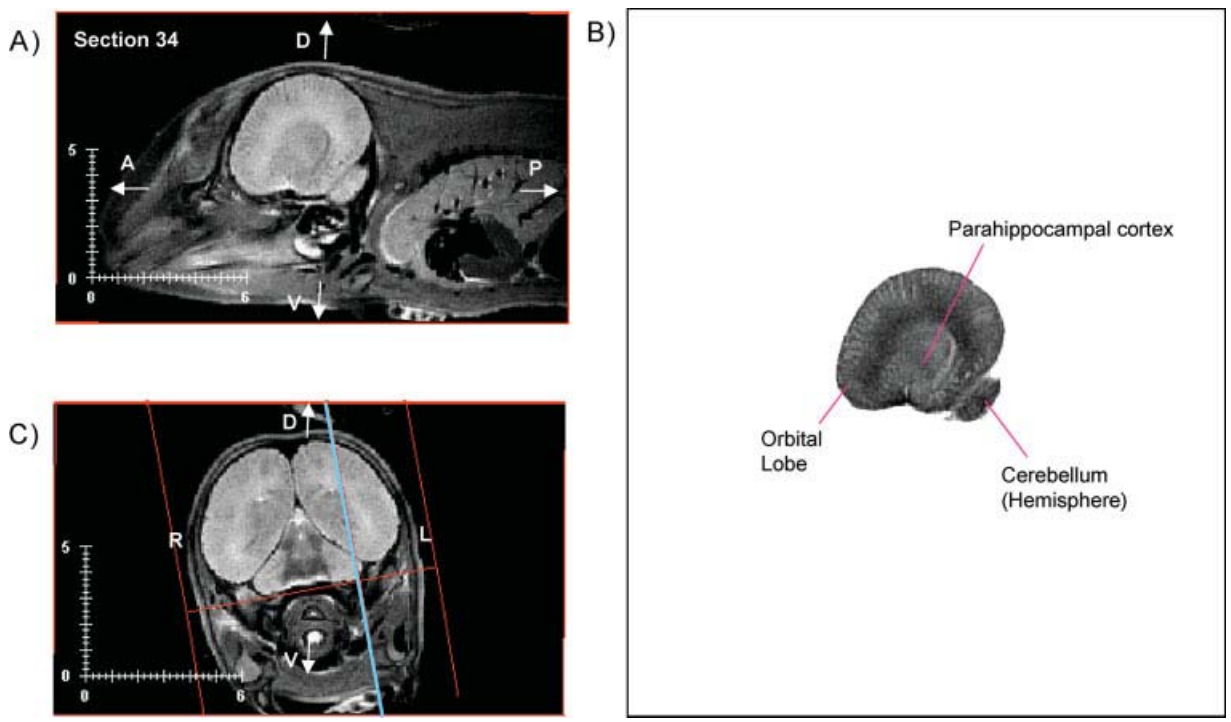

Figure 28. (Legend on page 1477)

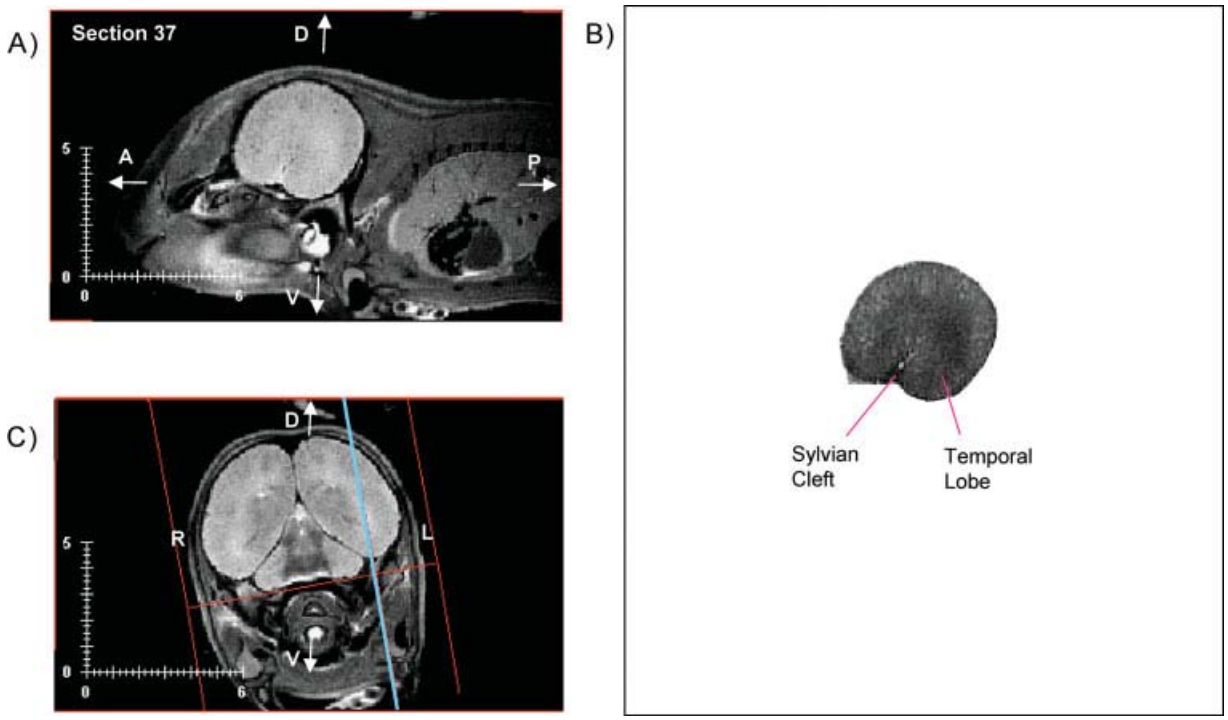

Figure 29.

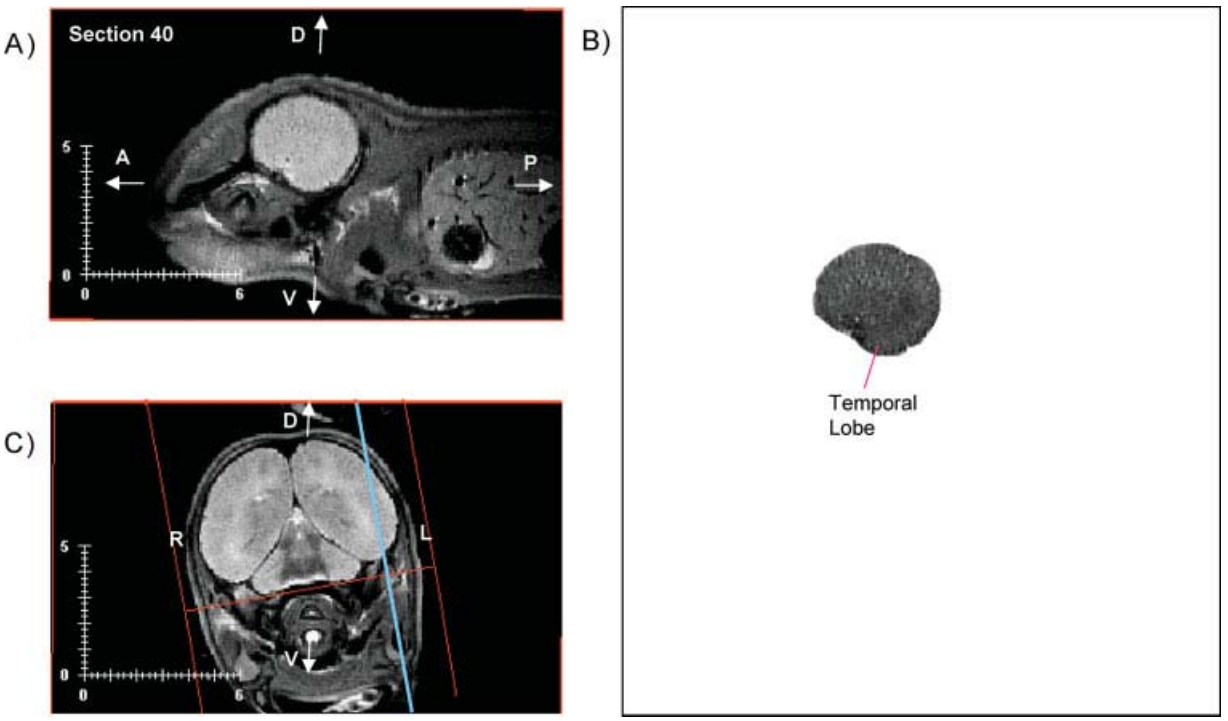

Figure 30.

Figures 25–30. Midline-to-lateral sequence of sagittal in situ magnetic resonance imaging (MRI) scans of the fetal brain. **A:** Native T2-weighted 2.0-mm-thick sagittal MRI brain sections of the left hemisphere at 6-mm intervals. **B:** Labeled brain excised from the head structure with the conventional MRI gray scale inverted. White matter appears white; gray matter appears gray; and cerebrospinal fluid appears black. **C:** Coronal MRI scans of the brain intact within the skull depicting the orientation of the section. Orange lines illustrate the span of the MRI sequence. Blue lines represent the plane of section. D, dorsal; V, ventral; L, left; R, right; A, anterior; P, posterior. Scale is in cm.

the caudate nucleus and the putamen) could be recognized in this fetus (Figs. 18B–21B). In addition, the hippocampus could be identified, contrary to a previous in situ MRI study of a fetal common dolphin preserved in formalin (Marino et al., 2001b). In our study, the hippocampal formation had already taken its characteristic tear-dropped shape, but was quite small relative to the overall size of the brain (Fig. 21B), similar to what was seen in the subadult. The corpus callosum was small (Figs. 20B–21B, 25B), as in the subadult. However, it appears to be myelinated at this stage of development.

Diencephalon. The large thalamus was easily recognized in the fetal MRI scans (Figs. 20B–21B, 25B–26B).

Mesencephalon. The inferior colliculus was well developed and already myelinated (Figs. 22B, 25B–26B). It had reached its subadult proportion and far exceeded the size of the superior colliculus.

Metencephalon and myelencephalon. Auditory pathways were easily observed at this fetal stage, including the cochlear nuclei (Fig. 22B), the trapezoid body (Figs. 25B–26B), and the lateral lemniscus (Figs. 22B, 26B). These structures were myelinated (i.e., appeared white in inverted T2 images). The cerebellum was large and well developed (Figs. 22B–24B, 25B–27B). It was heavily myelinated already. Hindbrain structures including the pons and inferior olive could be identified as could the spinal cord (Figs. 21B–24B, 25B) and were also heavily myelinated.

The myelination of axons is a critical phase during fetal brain development, because myelin is critical for normal axon function. A general principle in brain development is that structures that develop first in the brain become myelinated first. Myelin contains more lipids than proteins (70:30; as cited by Almajeed et al., 2004), which leads to a T2 hypointensity. In this study, the white matter tracts of the fetal hindbrain and cerebellum were prominent (Figs. 22B–24B, 25B). However, in the telencephalon, the white matter tracts were far less developed (Figs. 18B–24B, 26B–30B). In mammals, hindbrain structures develop and mature earlier than rostral brain structures (Allman, 1999). In addition, the white matter tracts of the auditory pathways in the fetal brains were myelinated, indicated by the T2 hypointensity signal of the inferior colliculus (Figs. 22B, 26B), the cochlear nuclei (Figs. 22B), and trapezoid body (Figs. 25B–26B). These findings provide evidence that hearing and auditory processing regions develop early during ontogeny, as described in previous odontocete studies (Solntseva, 1999). This is also true for humans, as reviewed in Ruben (1992) and Bappadityu et al. (2005). Montie et al. (2007) discuss the volumetric changes in white matter during ontogeny of the Atlantic white-sided dolphin in more detail.

CONCLUSIONS

This article presents the first anatomically labeled MRI-based atlas of the subadult and fetal brain of the Atlantic white-sided dolphin. It is different from previous MRI-based atlases of cetaceans in that it was created from images of fresh, postmortem brains in situ vs. brains that were removed and preserved in formalin. The close proximity of strandings to MRI facilities on Cape Cod and the quick response of personnel made this imaging possible. Because there are none of the potential distortions associated with the removal and fixation of the brain, we have a more realistic view of the brain, including its integrity, spatial relationships with head anatomy, and sizes of brain structures.

MRI studies of cetacean brains that were removed and preserved in formalin have been unable to identify the hippocampus, except in the killer whale (Marino et al., 2001a–c, 2003a,b, 2004a,b). In the MRI studies of formalin-fixed brains, the identification of the hippocampus in killer whales and the inability to identify the hippocampus in smaller odontocete species (e.g., beluga whale, spinner dolphin, dwarf sperm whale, harbor porpoise, and bottlenose dolphin) was most likely a function of the larger absolute size of the hippocampus in killer whales compared with the smaller size of the hippocampus in smaller odontocete species. It is somewhat puzzling that the hippocampus was visible in the in situ MRI scans of the Atlantic white-sided dolphins in this study and not the MRI scans of formalin fixed brains of other delphinid species (i.e., spinner dolphin and bottlenose dolphin). It is possible that severing the head and removing the brain, as was done in previous delphinid MRI studies, leads to the leakage of cerebrospinal fluid and therefore reduces the ability to perceive the hippocampus boundaries (note the fluid spaces around the hippocampus in Figs. 5 and 6). This possibility, in conjunction with the weight of the brain on the hippocampus and its potential thinning in the dorsal–ventral direction, may impede the visual perception of the hippocampal formation from MRI scans of formalin fixed brains.

In situ MRI scanning coupled with volumetric analysis may also allow a more accurate and reliable measure of the size of brain structures. This approach can be used not only as a tool to study brain evolution and developmental patterns in cetaceans but also to investigate the impacts of biological, chemical, and physical agents on marine mammal health (Montie, 2006). Environmental pollutants such as PCBs and PBDEs that bioaccumulate and biomagnify in cetaceans have been shown to affect the maturation of brain regions that depend on thyroid hormones in rodent species (Kimura-Kuroda et al., 2005; Sharlin et al., 2006). Domoic acid (a type of biotoxin produced by some diatom *Pseudo-nitzschia* species and associated with harmful algal blooms) has been shown to cause hippocampal atrophy in California sea lions (Silvagni et al., 2005). In situ MRI scanning, as a diagnostic tool with both postmortem specimens and live animals, sets the stage to use volumetric neuroimaging to investigate the impacts of emerging threats in the marine environment on marine mammal and human health.

ACKNOWLEDGMENTS

We thank the following past and present members of the Cape Cod Stranding Network for coordination and collection of specimens: Kristen Patchett, Betty Lentell, Brian Sharp, Kate Swails, Sarah Herzig, and Trish O'Callaghan. We are particularly thankful to Andrea Bogomolni and Dr. Michael Moore for assistance in necropsies. We are especially thankful to Scott Garvin, Rick

Rupan, Dr. Tin Klanjscek, Dr. Gareth Lawson, Dr. Regina Campbell-Malone, Dr. Joy Lapseritis, Paul Ryan Craddock, Tim Cole, Brendan Hurley, Misty Nelson, Brenda Rone, Brett Hayward, and Misty Niemeyer for assistance during specimen preparation and necropsies. We are especially thankful to Dr. Steven Sweriduk for allowing the use of the MRI scanner at Shields MRI and CT of Cape Cod. We are indebted to Julie Arruda, Scott Cramer, Dr. Iris Fischer, Bill Perrault, Terri Plifka, Cheryl Loring, and Rose Pearson for assistance during MRI scanning of specimens and data processing. We also thank Greg Early and Dr. Mark Baumgartner for helpful discussions. This study was conducted under a letter of authorization from Dana Hartley and the National Marine Fisheries Service Northeast Region, which allowed the possession of marine mammal parts. This study was supported through an Environmental Protection Agency STAR fellowship awarded to Dr. Eric Montie and a National Woman's Farm and Garden Association Scholarship awarded to Dr. Eric Montie.

LITERATURE CITED

Allman JM. 1999. Evolving brains. New York: Scientific American Library.

Almajeed AA, Adamsbaum C, Langevin F. 2004. Myelin characterization of fetal brain with mono-point estimated T1-maps. Magn Reson Imaging 22:565–572.

Bappaditya R, Roy TS, Wadhwa S, Roy KK. 2005. Development of the human fetal cochlear nerve: a morphometric study. Hear Res 202:74–86.

Conrad PA, Miller MA, Kreuder C, James ER, Mazet J, Dabritz H, Jessup DA, Gulland F, Grigg ME. 2005. Transmission of toxoplasma: clues from the study of sea otters as sentinels of *Toxoplasma gondii* flow into the marine environment. Int J Parasitol 35:155–1168.

de Boer J, Wester PG, Klamer HJ, Lewis WE, Boon JP. 1998. Do flame retardants threaten ocean life? Nature 394:28–29.

Evans AC; Brain Development Cooperative Group. 2006. The NIH MRI study of normal brain development. Neuroimage 30:184–202.

Jacobs MS, McFarland WL, Morgane PJ. 1979. The anatomy of the brain of the bottlenose dolphin (*Tursiops truncatus*). Rhinic Lobe (rhinencephalon): the archicortex. Brain Res Bull 4:1–108.

Kimura-Kuroda J, Nagata I, Kuroda Y. 2005. Hydroxylated metabolites of polychlorinated biphenyls inhibit thyroid-hormone-dependent extension of cerebellar Purkinje cell dendrites. Dev Brain Res 154:259–263.

Marino L. 1998. A comparison of encephalization between odontocete cetaceans and anthropoid primates. Brain Behav Evol 51:230–238.

Marino L, Murphy TL, Deweerd AL, Morris JA, Fobbs AJ, Humblot N, Ridgway SH, Johnson JI. 2001a. Anatomy and three-dimensional reconstructions of the brain of the white whale (*Delphinapterus leucas*) from magnetic resonance images. Anat Rec 262:429–439.

Marino L, Murphy TL, Gozal L, Johnson JI. 2001b. Magnetic resonance imaging and three-dimensional reconstructions of the brain of a fetal common dolphin, *Delphinus delphis*. Anat Embryol (Berl) 203:393–402.

Marino L, Sudheimer KD, Murphy TL, Davis KK, Pabst DA, McLellan WA, Rilling JK, Johnson JI. 2001c. Anatomy and three-dimensional reconstructions of the brain of a bottlenose dolphin (*Tursiops truncatus*) from magnetic resonance images. Anat Rec 264:397–414.

Marino L, Sudheimer K, Pabst DA, McLellan WA, Johnson JI. 2003a. Magnetic resonance images of the brain of a dwarf sperm whale (*Kogia simus*). J Anat 203:57–76.

Marino L, Sudheimer K, Sarko D, Sirpenski G, Johnson JI. 2003b. Neuroanatomy of the harbor porpoise (*Phocoena phocoena*) from magnetic resonance images. J Morphol 257:308–347.

Marino L, Sherwood CC, Delman BN, Tang CY, Naidich TP, Hof PR. 2004a. Neuroanatomy of the killer whale (*Orcinus orca*) from magnetic resonance images. Anat Rec A Discov Mol Cell Evol Biol 281:1256–1263.

Marino L, Sudheimer K, McLellan WA, Johnson JI. 2004b. Neuroanatomical structures of the spinner dolphin (*Stenella longirostris orientalis*) brain from magnetic resonance images. Anat Rec 279A:601–610.

McKinney MA, De Guise S, Martineau D, Beland P, Lebeuf M, Letcher RJ. 2006. Organohalogen contaminants and metabolites in beluga whale (*Delphinapterus leucas*) liver from two Canadian populations. Environ Toxicol Chem 25:30–41.

Montie EW. 2006. Approaches for assessing the presence and impact of thyroid hormone disrupting chemicals in delphinid cetaceans. PhD Thesis. Massachusetts Institute of Technology, Woods Hole Oceanographic Institution. p 303.

Montie EW, Ketten DR, Schneider G, Marino L, Touhey KE, Hahn ME. 2007. Volumetric neuroimaging of the Atlantic white-sided dolphin (*Lagenorhynchus acutus*) brain from in situ magnetic resonance images. J Comp Neurol (in preparation).

Morgane PJ, Jacobs MS, MacFarland WL. 1980. The anatomy of the brain of the bottlenose dolphin (*Tursiops truncatus*). Surface configurations of the telencephalon of the bottlenose dolphin with comparative anatomical observations in four other cetacean species. Brain Res Bull 5(Suppl):1–107.

Morgane PJ, Jacobs MS, Galaburda A. 1986. Evolutionary morphology of the dolphin brain. Dolphin cognition and behavior. In: Schusterman RJ, Thomas JA, Wood FG, editors. Dolphin cognition and behavior: a comparative approach. Hillsdale, NJ: Lawrence Erlbaum Associates. p 5–30.

Ridgway SH. 1990. The central nervous system of the bottlenose dolphin. In: Leatherwood S, Reeves R, editors. The bottlenose dolphin. San Diego: Academic Press. p 69–97.

Ridgway SH, Brownson RH. 1984. Relative brain sizes and cortical surface areas in odontocetes. Acta Zool Fennica 172:149–152.

Ruben RJ. 1992. The ontogeny of human hearing. Acta Otolaryngol 112:192–196.

Sandala GM, Sonne-Hansen C, Dietz R, Muir DCG, Valters K, Bennett ER, Born EW, Letcher RJ. 2004. Hydroxylated and methyl suflone PCB metabolites in adipose and whole blood of polar bear (*Ursus maritimus*) from East Greenland. Sci Total Environ 331:125–141.

Scholin CA, Gulland F, Doucette GJ, Benson S, Busman M, Chavez FP, Cordaro J, DeLong R, De Vogelaere A, Harvey J, Haulena M, Lefebvre K, Lipscomb T, Van Dolah FM, et al. 2000. Mortality of sea lions along the central California coast linked to a toxic diatom bloom. Nature 6765:80–84.

Sergeant DE, St. Aubin DJ, Geraci JR. 1980. Life history and Northwest Atlantic status of the Atlantic white-sided dolphin, *Lagenorhynchus acutus*. Cetology 37:1–12.

Sharlin DS, Bansal R, Zoeller RT. 2006. Polychlorinated biphenyls exert selective effects on cellular composition of white matter in a manner inconsistent with thyroid hormone insufficiency. Endocrinology 147:846–858.

Silvagni PA, Lowenstine LJ, Spraker T, Lipscomb TP, Gulland FMD. 2005. Pathology of domoic acid toxicity in California sea lions (*Zalophus californianus*). Vet Pathol 42:184–191.

Solntseva G. 1999. The comparison of the development of the auditory and vestibular structures in toothed whales -- beluga (Cetacea: Odontoceti - *Delphinapterus leucas*). Dokl Akad Nauk 364: 714–718.

Stephan H, Frahm H, Baron G. 1981. New and revised data on volumes of brain structures in insectivores and primates. Folia Primatol (Basel) 25:1–29.

Tarpley RL, Ridgway SH. 1994. Corpus callosum size in delphinid cetaceans. Brain Behav Evol 44:156–165.

US Department of Commerce and US Navy. 2001. Joint interim report: Bahamas marine mammal stranding event of 15–16 March 2000. Available at: http://www.nmfs.noaa.gov/prot_res/overview/Interim_Bahamas_Report.pdf.